

DEHYDRATION OF APPLE RINGS

by

RICHARD HENRY GEORGE PROMNITZ

SUBMITTED IN FULFILMENT OF
THE REQUIREMENTS OF THE
DEGREE OF
MASTER OF SCIENCE
IN THE ENGINEERING FACULTY
OF THE UNIVERSITY OF CAPE TOWN.

APRIL, 1971.

The copyright of this thesis is held by the
University of Cape Town.
Reproduction of the whole or any part
may be made for study purposes only, and
not for publication.

The copyright of this thesis vests in the author. No quotation from it or information derived from it is to be published without full acknowledgement of the source. The thesis is to be used for private study or non-commercial research purposes only.

Published by the University of Cape Town (UCT) in terms of the non-exclusive license granted to UCT by the author.

A B S T R A C T

The effect of air humidity and velocity, tray surface and ring thickness, on the drying rates of apple rings, is reported. Drying rates for different apple slice thicknesses are correlated with the total moisture content of the fruit and the air relative humidity.

Also reported are results on the simulation, both experimental and computational, for the parallel-flow industrial dehydrator drying process.

A C K N O W L E D G E M E N T S

Firstly, the author would like to express his sincere appreciation to his supervisors, Professor A. D. Carr and Dr. H. O. Buhr, for the generous and unselfish assistance they gave him throughout the duration of his research work, which has culminated in the submission of this thesis.

The author also wishes to thank Dr. A. C. Visser of the Food Technology Department, Stellenbosch, for advice offered and interest shown in this investigation.

On the technical staff, the author would especially like to thank Mr. K. E. Wheeler and Mr. A. Jacobs for work they did for him in making various components of the experimental equipment.

Furthermore, the author is grateful to Molteno Brothers of Grabouw for supplying the fresh fruit for the experimental work, and to the South African Dried Fruit Corporation for the loan of the Hassia Apple Peeling and Coring Machine.

Finally, the author wishes to extend his sincere thanks to the C.S.I.R. for their generous financial assistance.

TABLE OF CONTENTS

	<u>PAGE NO.</u>	
ABSTRACT	ii	
ACKNOWLEDGEMENTS	iii	
TABLE OF FIGURES	vi	
<u>CHAPTER 1</u>	<u>GENERAL INTRODUCTION AND DISCUSSION OF THE</u>	
	<u>INDUSTRIAL DEHYDRATOR</u>	1
1.1	General Introduction	1
1.2	The Industrial Tunnel Dehydrator	2
<u>CHAPTER 2</u>	<u>DRYING THEORY</u>	5
2.1	Introduction to Basic Concepts and Definitions	5
2.2	Heat Transfer	5
2.3	Drying under Constant External Conditions	5
2.4	Model used to Describe the Drying of Apple Rings	6
<u>CHAPTER 3</u>	<u>EQUIPMENT</u>	8
3.1	Description of Wind Tunnel	8
3.2	Air Distribution in Drying Section	8
3.3	Air Movement, Measurement and Control	11
3.4	Weighing System	11
3.5	Dry-Bulb Measurement and Control	14
3.6	Wet-Bulb Measurement and Control	15
3.7	Temperature Recording	15
3.8	Electrical Systems	18
<u>CHAPTER 4</u>	<u>EXPERIMENTAL PROCEDURE</u>	20
4.1	Introduction	20
4.2	Preparation of Apple Rings	20
4.3	General Operational Procedure of the Wind-Tunnel	22
4.4	Equilibrium Curve	22
4.5	Drying Rate Curves	23
4.6	Simulation Runs	25
4.7	Moisture Content Analysis	26

	<u>PAGE NO.</u>
<u>CHAPTER 5</u> <u>RESULTS</u>	28
5.1 Introduction	28
5.2 Equilibrium Curve	28
5.3 Drying under Constant External Conditions	30
5.4 The Influence of Humidity on Drying Rates	32
5.5 The Effect of Apple Thickness on Drying Rates	36
5.6 Comparison of Open and Solid Tray Surfaces	39
5.7 The Effect of Velocity on Drying Rates	39
5.8 Constant-Rate Drying	42
5.9 Investigation into the Effect of Finite Packed Length of Apple Rings on an Assumption of Point-Drying Conditions	42
5.10 Simulation Runs	47
5.11 Application of the Results obtained under Constant External Drying Conditions	48
<u>CHAPTER 6</u> <u>CONCLUSIONS AND RECOMMENDATIONS</u>	52
6.1 Conclusions	52
6.2 Recommendations	52
 NOMENCLATURE	 54
 LIST OF REFERENCES	 56
 APPENDICES	 57
<u>APPENDIX A</u> <u>EQUILIBRIUM MOISTURE CONTENT DATA</u>	A-1
<u>APPENDIX B</u> <u>CALCULATION OF TOTAL MOISTURE CONTENT</u>	B-1
B.1 Sample Calculation used in Moisture Content Analyses	B-1
B.2 Calculation of Total Moisture Content of Apple Rings during Drying	B-1
<u>APPENDIX C</u> <u>DRYING RATE COMPUTATION AND TABULATION</u>	C-1
C.1 Sample Calculation of Drying Rate	C-1
C.2 Tabulation of Drying Rate Results	C-2
<u>APPENDIX D</u> <u>EXPLANATION OF THE COMPUTER PROGRAM USED TO SIMULATE THE DEHYDRATOR DRYING PROCESS</u>	D-1

FIGURES

	<u>PAGE No.</u>
<u>Fig. 1</u> Parallel-Flow Industrial Tunnel Dehydrator	3
<u>Fig. 2</u> Essential Features of the Wind Tunnel used in Experimental Work.	9
<u>Fig. 3</u> <u>Wind-Tunnel Used in Experimental Work.</u>	10
1. Wet- and dry-bulb contact thermometers	
2. Top-loading precision balance	
3. Drying section	
4. Honeycomb	
5. Gauze screen	
6. Vane turns	
7. Electrical resistance heating bars	
8. Turbine-type centrifugal fan	
9. Variable constriction	
<u>Fig. 4</u> <u>Drying Section Cartridge with Tray used for Drying under Constant External Conditions</u>	12
1. Top-loading precision balance	
2. Steel structure supporting the tray	
3. Drying section lid	
4. Steel frame with plastic-coated wire tray surface	
<u>Fig. 5</u> <u>Drying Section Cartridge with Trays used in Simulation Runs.</u>	13
1. Top-loading precision balance.	
2. Steel structure to support the middle tray	
3. Drying section lid	
4. Plastic-coated wire tray used in industrial dehydrator simulation runs.	
<u>Fig. 6</u> <u>Wet- and Dry-Bulb Temperature Measuring Systems</u>	16
1. Distilled water reservoir	
2. Dry-bulb contact thermometer	
3. Wet-bulb contact thermometer	
4. Air pipe and water feed pipe	
<u>Fig. 7</u> Wet-Bulb Temperature Measuring System.	17
<u>Fig. 8</u> Circuitry for A.C. Power Input to Wet- and Dry-Bulb Temperature Control Systems.	19
<u>Fig. 9</u> Apple Peeling and Coring Machine	21
<u>Fig. 10</u> Layout of Apple Rings Packed on the Tray for Drying Under Constant External Conditions.	24.

	<u>PAGE NO.</u>
<u>Fig. 11</u> Equilibrium Moisture Content Curve of 6.4 mm Thick Apple Ring Slices.	29
<u>Fig. 12</u> Drying Curve of 6.4 mm Thick Apple Ring Slices at 30 Percent Relative Humidity.	31
<u>Fig. 13</u> The Effect of Humidity on the Drying Rate of 6.4 mm Thick Apple Ring Slices.	34
<u>Fig. 14</u> Normalized Drying Rate Curve for 6.4 mm Thick Apple Ring Slices - Eqn. (10).	35
<u>Fig. 15</u> The Effect of Apple Ring Slice Thickness on Drying Rates at 20 Percent Relative Humidity.	37
<u>Fig. 16</u> The Effect of Apple Ring Slice Thickness on Drying Rates at 20 Percent Relative Humidity.	38
<u>Fig. 17</u> The Effect of Tray Surface on Drying Rates of 6.4 mm Thick Apple Ring Slices at 40 Percent Relative Humidity.	40
<u>Fig. 18</u> The Effect of Tray Surface on Drying Rates of 6.4 mm Thick Apple Ring Slices at 20 Percent Relative Humidity.	41
<u>Fig. 19</u> The Ratio of Drying Rates obtained on the Solid Tray Surface to Those on the Plastic-Coated, Wire Tray surface (for 20 and 40 Percent Relative Humidity).	41
<u>Fig. 20</u> The Effect of Air Velocity on the Drying Rates of 6.4 mm Thick Apple Ring Slices at 20 Percent Relative Humidity.	43
<u>Fig. 21</u> The Effect of Air Velocity on the Drying Rates of 6.4 mm Thick Apple Ring Slices at 40 Percent Relative Humidity.	
<u>Fig. 22</u> Drying Rates determined at High Apple Ring Moisture Contents (6.4 mm Thick Slices), in an Attempt to show Constant-Rate Drying.	45
<u>Fig. 23</u> Curves showing the Effect of Packed Length on the Drying Rates of 6.4 mm Thick Apple Ring Slices at 10 Percent Relative Humidity.	46
<u>Fig. 24</u> Input and Output Temperatures to and from Trays in Different Positions in the Simulated Tunnel, found by Computational and Experimental Simulation of the Industrial Drying Process.	51

CHAPTER 1

GENERAL INTRODUCTION AND DISCUSSION OF THE INDUSTRIAL DEHYDRATOR

1.1 GENERAL INTRODUCTION.

Dehydration plays an important role in the preparation of food products.

Until about 60 years ago fruit was dried almost exclusively in the sun. This sun-drying technique essentially involves the preparation of the fruit, the spreading out of the fruit on trays which are then placed in the sun, to allow drying by solar energy. Fruits such as raisins, apricots, peaches and pears are still primarily dried in the sun. A more modern innovation is the dehydrator, which is a mechanical means of drying* fruit.

There are a number of advantages which favour dehydration as a method of drying, in preference to sun-drying [1]. Sun-dried fruit, placed on trays, is susceptible to insect infestation; contamination with micro-organisms which may cause moulding and fermentation; dust and dirt contamination, and damage caused by rain and animals. Sun-drying is slow, resulting in great losses of the sulphur dioxide preservative from the treated fruit. Dehydration, if properly controlled, protects against all of these hazards and produces clean fruit of higher quality. The dehydration process generally requires a much smaller working area than the sun-drying process, is less labour intensive and requires fewer trays since the turnover of trays is higher. On the other hand, inefficient or improper operation of dehydrators may be costly, or may give rise to an inferior product.

Fruit is generally dehydrated either by means of tunnel dehydrators, cabinet, drum or spray dryers or in kilns [2]. In the Western Cape numerous tunnel dehydrators have been constructed to process a portion of the deciduous fruit crop.

* Throughout this text the words "dried" and "dehydrated" will be assumed analogous; any reference to produce dried in the sun, will be termed sun-dried.

This thesis covers an experimental investigation into the drying of apple rings, with a view to obtaining information such as rates of drying, on which the design and operation of industrial dehydrators may be based.

1.2 THE INDUSTRIAL TUNNEL DEHYDRATOR [4].

In the fruit industry of the Western Cape the single tunnel dehydrator is more extensively used than any other type of drier. A diagram of this type of drier is shown in Fig. 1 [3].

The salient features, as depicted in Fig. 1, of the single tunnel dehydrator are: the drying and air recirculation sections, the fan, the air heating system, the trucks and trays, and the instrumentation and control systems.

The tunnel dehydrator is normally constructed of brick, with the tunnel long enough to accommodate 10 trucks loaded with drying trays. Trays, which are usually of standard dimensions, 0.915 m by 1.830 m, are built of wood. This type of tray complies quite favourably with the following requirements: trays must be easy to fabricate, inexpensive, easily scraped clear of adhering dried material, light but strong and rigid, and the tray must not contaminate the produce [5]. However, the wooden tray has the drawback in that, since the tray is virtually solid, the total surface area of the drying fruit, exposed to the drying air, is curtailed. This is especially applicable to the drying of apple rings, when the flat ring is laid on the wooden surface.

The trays, covered with fruit, are stacked on the trucks to a height of about 1.5 to 2.1 m, depending on the tunnel height. Between each tray is a spacing of approximately 80 mm, which allows for unobstructed flow of the circulating air. The trucks are pushed into one side of the tunnel and others, containing the dried product, are removed from the opposite end. Thus the tunnel operates in a quasi-continuous fashion, since each truck remains stationary for one tenth of the total drying time, in each of the 10 positions along the tunnel.

It is essential that the fan produces a good, uniform air distribution in the tunnel free cross-sectional area. This facilitates

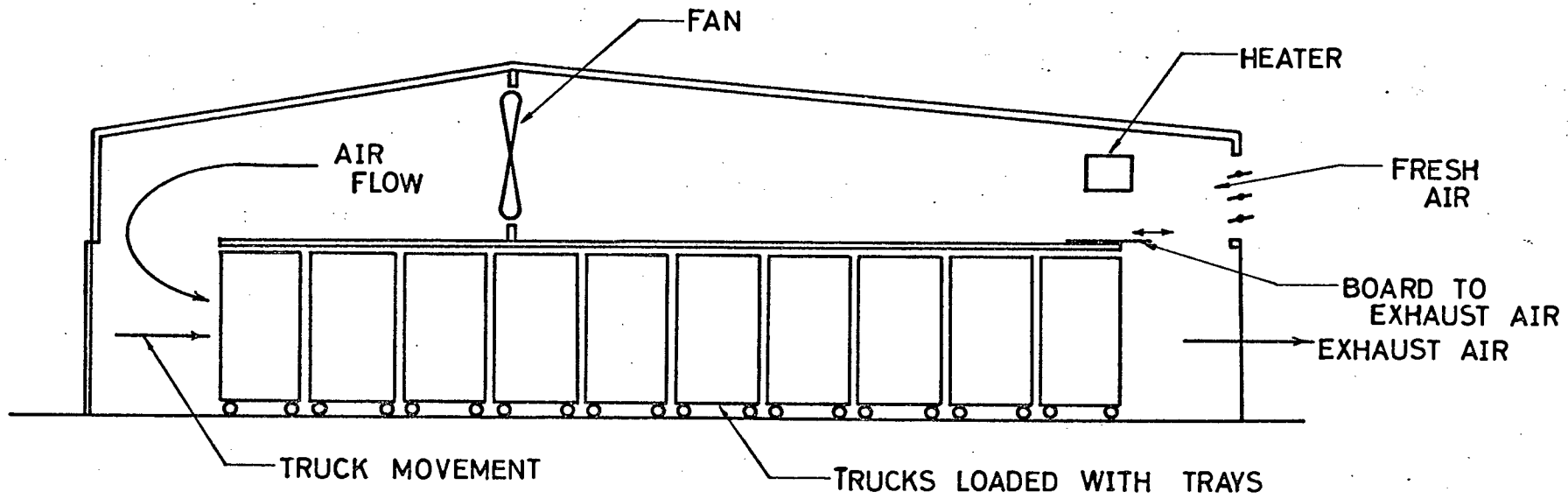


Fig. 1

Parallel-Flow Industrial Tunnel Dehydrator.

even heat and mass transfer to and from the drying fruit. The required air velocity for drying fruit, is dictated by the variety of fruit being dried (it is usually an economic consideration). For apple rings, for example, a lineal velocity of about 240m/min is desirable. Parallel and counter-current flow modes of operation may be used in a tunnel of this nature. Parallel flow operation, where the air flows in the same direction as the truck movement, has the advantage in that the hottest air contacts the wettest material. This is often useful since the evaporative cooling effect of the water leaving the wet fruit allows the use of higher air temperatures than would be the case for counter-current operation. On the other hand, since the cooler, moist air contacts the final product, it is more difficult to achieve a low, final moisture content in the parallel flow situation. The reverse is the case for counter-current operation, because the hottest air comes into contact with the driest material.

Since little heat is either added or lost from the tunnel, the system is practically adiabatic, with the result that the wet-bulb temperature is almost invariant along the entire length of the tunnel. The maximum air dry-bulb temperature allowable, for drying, is determined by the type of fruit being dried, but the common denominator is that the temperatures used must not cause any damage to the fruit.

The air is heated either directly, by circulating the products of combustion of oil or gas fuel with the drying air; or indirectly, where heat from steam or combustion gases is transferred to the drying air, using a heat exchanger. Direct heating by burning a gas fuel is often preferable. This is so because there is no danger of contaminating the product with soot, allows for easy control (of dry-bulb temperature), and it is invariably a more economic means of heating than indirect heat transfer.

Humid air is exhausted from the dehydrator and fresh air added, by obstructing the air passage between the exhaust and inlet openings, as shown in Fig. 1, and thus forcing the required volume of air out of the dehydrator. The amount of air exhausted is an economic consideration, since this air carries with it a certain quantity of heat.

CHAPTER 2

- DRYING THEORY -

2.1 INTRODUCTION TO BASIC CONCEPTS AND DEFINITIONS

From the nature and shape of apple rings, it should be realized, that an exact mathematical description, of the mechanism of the drying process of apple rings, could be complex and cumbersome to work with. For this reason a semi-empirical approach has been adopted, in this work, to describe and correlate various factors involved in drying.

Some definitions on the measure of moisture content, in a solid, are given below.

The equilibrium moisture content is the amount of water contained in a product, once it has equilibrated with its environment [6]. The equilibrium moisture content is usually described in terms of g water/g bone-dry solid, X_T^* .

The total moisture content of a solid is denoted by X_T , and any moisture in excess of the equilibrium moisture content is termed the free moisture content, X .

$$X = X_T - X_T^* \quad (1)$$

The minimum amount of water, in a substance, required to exert the vapour pressure of pure water, at the air temperature, and any moisture level lower than that, is termed bound water. Unbound water is water, in a substance, which can exert the vapour pressure of water at the air temperature (i.e. it is any water in excess of the maximum level of bound water). With apple rings, for example, the superficial water found on the rings after preparation would be unbound water.

2.2 HEAT TRANSFER

In forced convection dryers, such as the tunnel dehydrator, heat is transferred, to the drying material, primarily by convection. Conductive and radiant heat transfer is generally insignificant.

2.3 DRYING UNDER CONSTANT EXTERNAL CONDITIONS

Non-hygroscopic solids have extended constant-rate drying periods, when unbound moisture is lost [7]. This is followed by falling rate period, where drying rate decreases with a decrease in

the bound water. These constant-rate drying periods are usually well defined and easily measured experimentally (e.g. drying of wet sand-beds etc.). In contrast, with the drying of hygroscopic solids (such as apple rings), only careful experimental work may manifest a short period of constant-rate drying. Often the rate begins to decrease as soon as drying starts [8].

2.4 MODEL USED TO DESCRIBE THE DRYING OF APPLE RINGS

In an investigation of this nature, it is desirable to obtain a single, normalized drying rate curve which will characterize the drying of a specific material under, say, different driving forces. This is a good way of correlating data and also provides a convenient means of applying results for design purposes. Bearing this in mind, a model was postulated in this work, to describe the drying of apple rings, and is given below:

Before the model is developed, two concepts, namely the resistance to mass transfer, R , and the driving force, D.F., need introduction:

With forced convection, where high air flow rates are used, a considerable amount of mixing and turbulence exists with the result that the controlling resistance to mass transfer may be assumed not to be in the gas phase, but rather as a diffusional resistance in the solid phase. In normal pipe flow, the frictional resistance of the wall increases with the rate of fluid throughput. The diffusional resistance of water through the apple rings may be assumed to increase analogously, with the rate of water loss, $\frac{dw}{dt}$. Furthermore, since the texture of the apple rings, varies with total moisture content, X_T , the resistance to diffusion is also probably a function of this variable.

$$\therefore R = F\left(X_T, \frac{dw}{dt}\right) \quad (2)$$

As a first approximation, the diffusional resistance is assumed to be proportional to the power n of the drying rate and to the power c of the total moisture content.

$$\therefore R = a\left(\frac{dw}{dt}\right)^n X_T^c \quad (3)$$

The driving force, D.F., is given by the difference between the potential equilibrium vapour pressure of the apple ring, p^* , and the partial pressure of the water in the drying air, p . In this context, p^* , is the theoretical vapour pressure that an apple ring would exert at equilibrium, if it had a total moisture content of X_T .

$$\therefore \text{D.F.} = p^* - p \quad (4)$$

Eqn. (4) may be expressed in terms of the saturation vapour pressure, p_s , of water at the air temperature, the percentage relative humidity of the air, H_r , and the corresponding value of percentage relative humidity, H_r^* , which results in the equilibrium vapour pressure, p^* .

$$\therefore \text{D.F.} = 0.01(H_r^* - H_r)p_s \quad (5)$$

A generalized expression for rate is:

$$\text{Rate} = \frac{\text{Driving Force}}{\text{Resistance}} \quad (6)$$

Thus the rate of evaporation of water, $\frac{dw}{dt}$, from the surface of the apple rings is given by Eqns. (3), (5) and (6):

$$\frac{dw}{dt} = \frac{[0.01(H_r^* - H_r)p_s]}{a\left(\frac{dw}{dt}\right)^n X_T^c} \quad (7)$$

$$\text{or} \quad \left(\frac{dw}{dt}\right)^{n+1} = \frac{1}{a}[0.01(H_r^* - H_r)p_s]X_T^{-c}$$

$$\therefore \frac{dw}{dt} = \left[\frac{1}{a} 0.01(H_r^* - H_r)p_s X_T^{-c}\right]^{1/n+1}$$

$$\therefore \text{say } \frac{dw}{dt} = A[0.01(H_r^* - H_r)p_s]^B X_T^C \quad (9)$$

$$\text{or} \quad \frac{\frac{dw}{dt}}{[0.01(H_r^* - H_r)p_s]^B} = A X_T^C \quad (10)$$

The significance of Eqn. (10) is:

If the approximations hold, it should be possible to normalize the drying rates obtained for different driving forces, to a single curve, by an expression of the form of Eqn. (10).

The applicability of this relation to the results obtained in this investigation, is discussed in sections 5.4 and 5.5.

CHAPTER 3.

EQUIPMENT

3.1 DESCRIPTION OF WIND-TUNNEL

A wind-tunnel, shown in Fig. 2, with a centrifugal fan circulating heated air, formed the basic unit used in experimental work. The system had facilities to institute the control of wet- and dry-bulb temperatures, by controlling the power input to immersion heaters and electrical resistance heating bars respectively.

The tunnel, which was primarily constructed of plywood, had an overall length of 2.44 m., a height of 1.07 m. and a width of 0.46 m. The drying section, in which the fruit was dried, had a total length of 1.27 m., a height of 0.30 m., and a width of 0.46 m. The different types of trays, on which the apple rings were dried, were inserted into the drying section and the weight of the fruit obtained using a top-loading type balance.

3.2 AIR DISTRIBUTION IN DRYING SECTION

Since the rate of drying of fruit is a function of air velocity, in order to characterize drying, a uniform velocity throughout the cross-section of the drying section is necessary. Although the entrance length of the drying section was curtailed by the total practicable length of the wind-tunnel, an improved air distribution was achieved by the insertion of a number of guide vanes, honeycombs and a resistance to air flow.

Guide vanes, which were constructed of 22 gauge galvanized steel sheeting, were used in three of the tunnel corners, as illustrated in Fig. 2. Their principal function was to reduce the resistance to air flow around the corners [9]. The vanes situated at the fan outlet play an important part in the initial distribution of the air from the fan; these vanes were positioned so as to produce the optimum air distribution in the drying section.

To straighten air flow and to reduce swirl, two honeycombs were used, one before, and the other after the drying section. The honeycombs have 25 mm. square cells, with an axial length of 100 mm. They were designed according to B.S.I. specifications [10] and

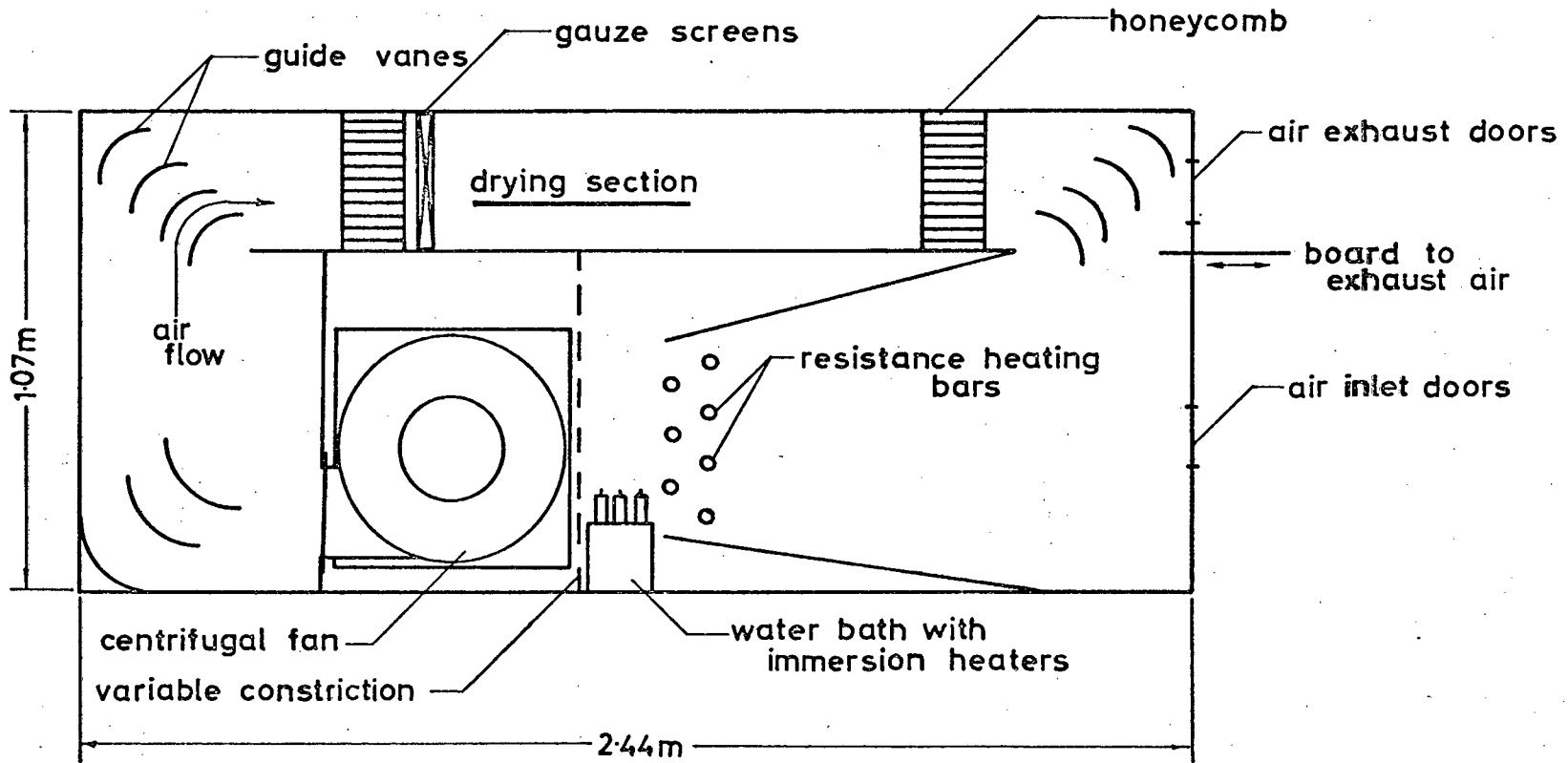


Fig. 2 Essential Features of the Wind Tunnel used in Experimental Work.

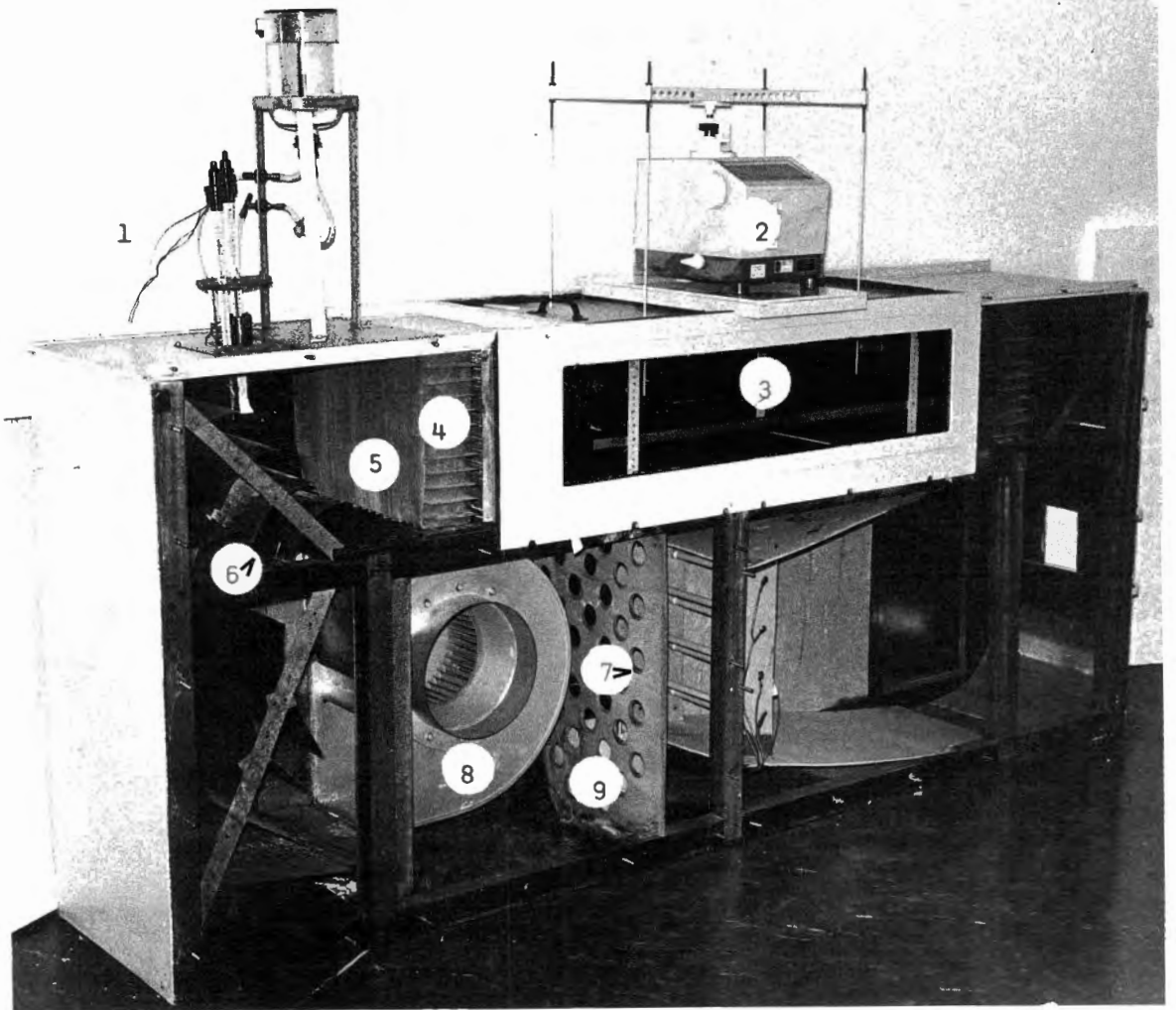


Fig. 3 Wind-tunnel used in Experimental Work.

1. Wet- and dry-bulb contact thermometers.
2. Top-loading precision balance.
3. Drying section.
4. Honeycomb.
5. Gauze screen.
6. Vane turns.
7. Electrical resistance heating bars.
8. Turbine-type centrifugal fan.
9. Variable constriction.

constructed of 22 gauge steel sheeting.

Three 36 mesh stainless-steel gauze screens (arranged in series), presented a resistance to air flow and facilitated the redistribution of the air before it entered the drying section. In addition to the production of a more favourable velocity profile (i.e. approaching plug-flow), wire gauze tends to reduce swirl [11].

3.3 AIR MOVEMENT, MEASUREMENT AND CONTROL

Air was circulated by a turbine-type centrifugal fan, rate to deliver $48.1 \text{ m}^3/\text{min}$. at 25 mm. water gauge. The 0.71 kw. fan motor was situated outside the wind-tunnel and coupled to the fan by a shaft.

Air velocity was measured with a pitot tube, mounted on one side of the drying section - this allowed for horizontal and vertical traverse. The differential across the pitot tube was converted to an electrical output by means of a pressure transducer with a range of ± 35 mm. water gauge. The signal from the transducer was then amplified and recorded on a pen recorder.

A variable constriction, as shown in Fig. 3, was used to control the air velocity. Manual control was effected by changing the resistance to air flow of the constriction, which essentially consisted of two plywood boards with coinciding 50 mm. holes. Movement of the one board in relation to the other, constricted these holes which thus decreased the free cross-sectional area for air flow.

Two sets of sliding doors, as illustrated in Fig. 2, enable continuous exhausting and replacement of any desired portion of the circulating air. This was done by introducing a pressure drop between these two sets of doors, in the form of a sliding plywood board.

3.4 WEIGHING SYSTEM

The tray on which the apple rings were spread was suspended below a top-loading precision balance (SARTORIUS, model 2250, 7 kg. max. loading) as shown in Fig. 4. This whole cartridge-type structure fitted snugly into the drying section, as shown in Fig. 3. By rotating a knurled knob which was on a screw pitch, the tray could be brought into its elevated weighing position, as depicted in Fig. 4. Sufficient

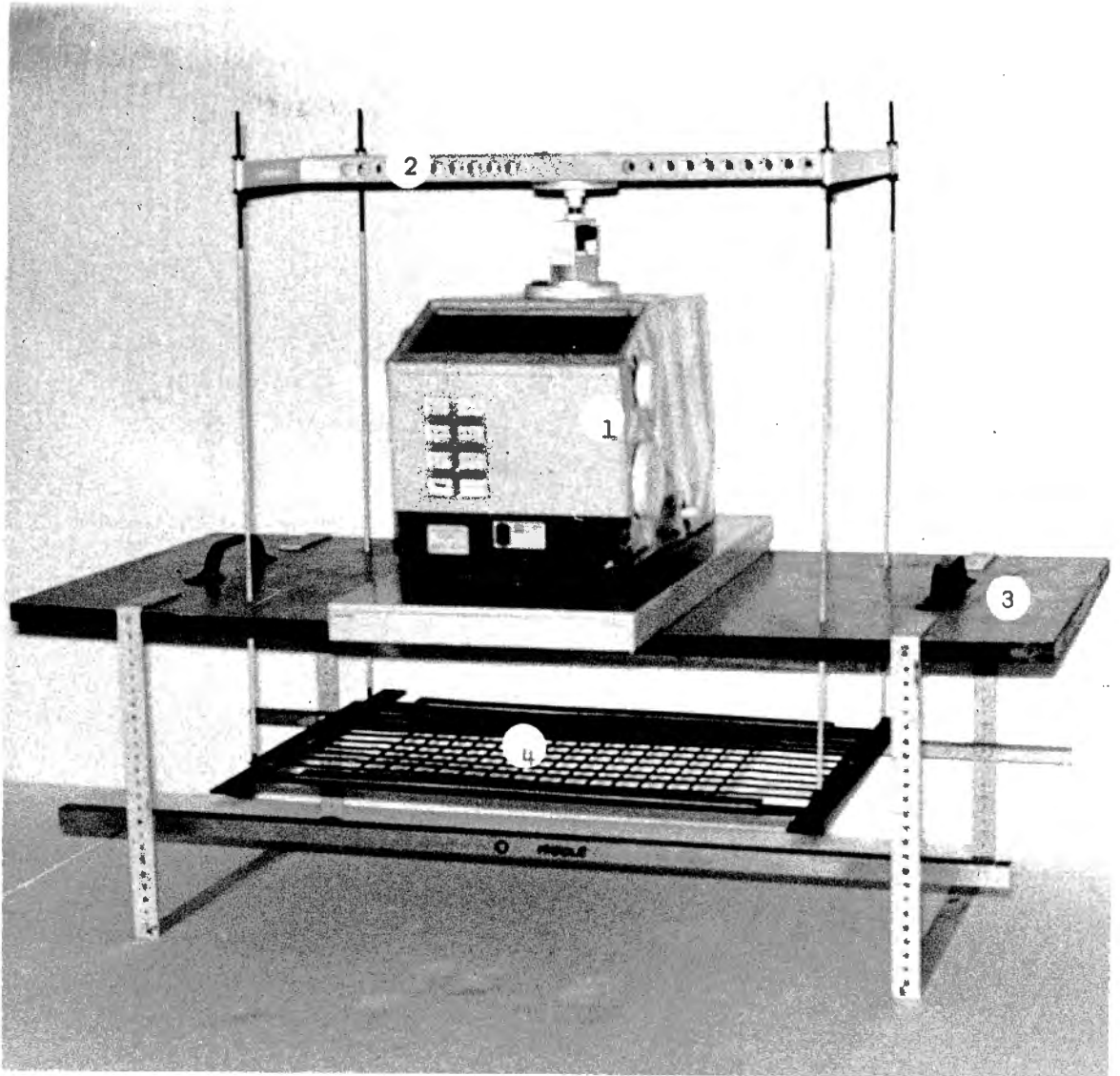


Fig. 4 Drying Section Cartridge with Tray used for drying under Constant External Conditions.

1. Top-loading precision balance.
2. Steel structure supporting the tray.
3. Drying Section lid.
4. Steel frame with plastic-coated wire tray surface.

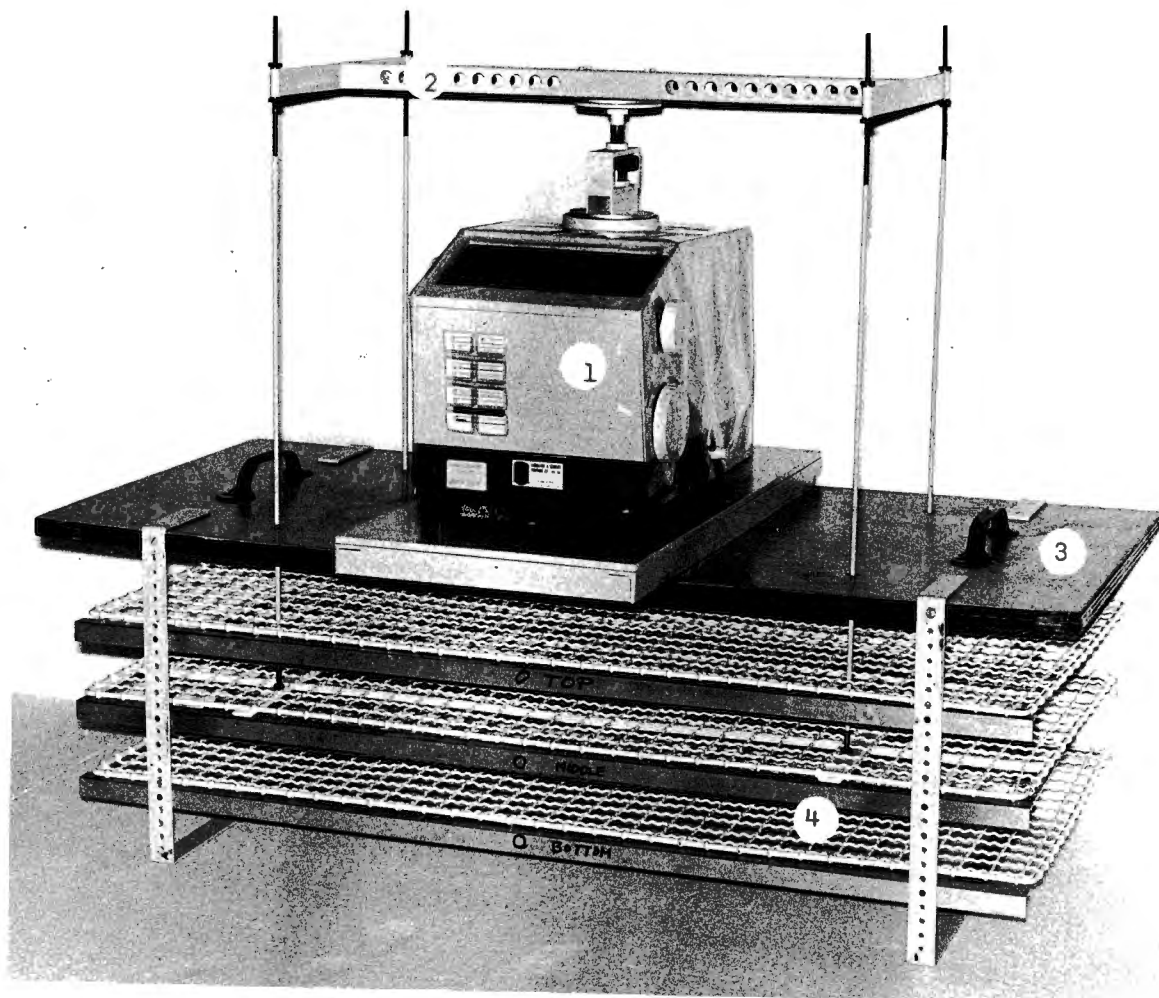


Fig. 5 Drying Section Cartridge with Trays used in Simulation Runs.

1. Top-loading precision balance.
2. Steel structure to support the middle tray.
3. Drying Section lid.
4. Plastic-coated wire tray used in industrial dehydrator simulation runs.

tolerance was provided for the rods, passing through the cartridge lid and for the tray in the drying section, to facilitate easy and quick weighing of the load on the tray.

The steel structure, shown in Fig. 4, on to which any tray surface could be attached was used for experimental work done under constant drying conditions. Two types of tray surface were tested in this work, they were: a plastic-coated wire surface (with 25 mm. square mesh) and a solid tray surface made of a 1.5 mm, thick plastic laminate (tradename - PANALYTE). For experimental work done on simulating the industrial dehydrator, a tray arrangement was used as shown in Fig. 5. These three plastic-coated, wire trays had dimensions of: 0.91 m. by 0.45 m. The length of 0.91 m. was chosen so as to duplicate the length of standard industrial dehydrator trays, while the width of the tray, 0.45 m., was considered to produce sufficient resultant area, to enable a reliable representation of a tray section, as found in an industrial dehydrator (using the same type of tray).

Once installed, trays were accessible through a hinged door positioned at the side of the tunnel, opposite the observation window.

3.5 DRY-BULB MEASUREMENT AND CONTROL

The dry-bulb temperature was controlled by means of a contact thermometer, placed immediately before the drying section, as shown in Fig. 3. Heat loss, between the dry bulb temperature sensing point and the drying section was calculated as well as found to be minimal (since the contact thermometer reading was very close to that of a thermocouple placed at the drying section outlet - i.e. in the absence of a drying load of fruit).

The contact thermometer activated relays, which, in turn allowed power input to those of the 7 x 1 kw heating bars that were switched to the control mode of operation - the circuitry of this control system is dealt with in section 3.8.

When controlling about a constant set point, this dry-bulb control system was very effective, since it controlled the temperature to $\pm 0.2^{\circ}\text{C}$ of the set point. The factor contributing mainly to this error was the relatively large time constant of the dry-bulb contact

thermometer (due to the large volume of mercury in the thermometer bulb), resulting in its slow response to temperature fluctuation.

3.6 WET-BULB MEASUREMENT AND CONTROL

Wet-bulb temperature control was effected by means of a contact thermometer which was operated as a wet-bulb measuring device. This system, as shown in Fig. 6, was also placed before the drying section. The bulb of the contact thermometer was covered with a muslin sock, which dipped into a copper trough containing distilled water - the diagram, given in Fig. 7, shows the wet-bulb system used. The most satisfactory height for the thermometer bulb to be above the water was approximately 20 mm; this allowed the water travelling up the muslin cloth, by capillarity, sufficient time to equilibrate, with the heated air, to the wet-bulb temperature. The water in the trough was replenished by gravitational flow. As soon as the water level in the trough fell below the hole drilled in the air pipe, air escaped up the air-pipe and into the reservoir, thus allowing water to flow down the feed pipe. This system worked adequately. It should be noted that the use of a single pipe to the water reservoir, to allow for both water and air passage, was found to be impracticable, since the system so formed was unstable, causing the water level in the trough to oscillate violently.

The contact thermometer activated a relay which allowed power input to immersion heaters in a water bath. The electrical and control circuitry was identical to that used for the dry-bulb control system and is discussed in section 3.8. Two 1 kw and a 0.6 kw immersion heater were used to produce steam. They had to be cleaned off, periodically, to remove scale. A constant-head reservoir, outside the tunnel, kept the water bath supplied with tap water.

When the wet-bulb temperature was controlled about a static set-point, under steady state conditions, this control system controlled to within $\pm 0.4^{\circ}\text{C}$ of the set-point.

3.7 TEMPERATURE RECORDING

A multipoint temperature recorder was capable of measuring and recording 12 temperatures within the range of 0 to 120°C . The

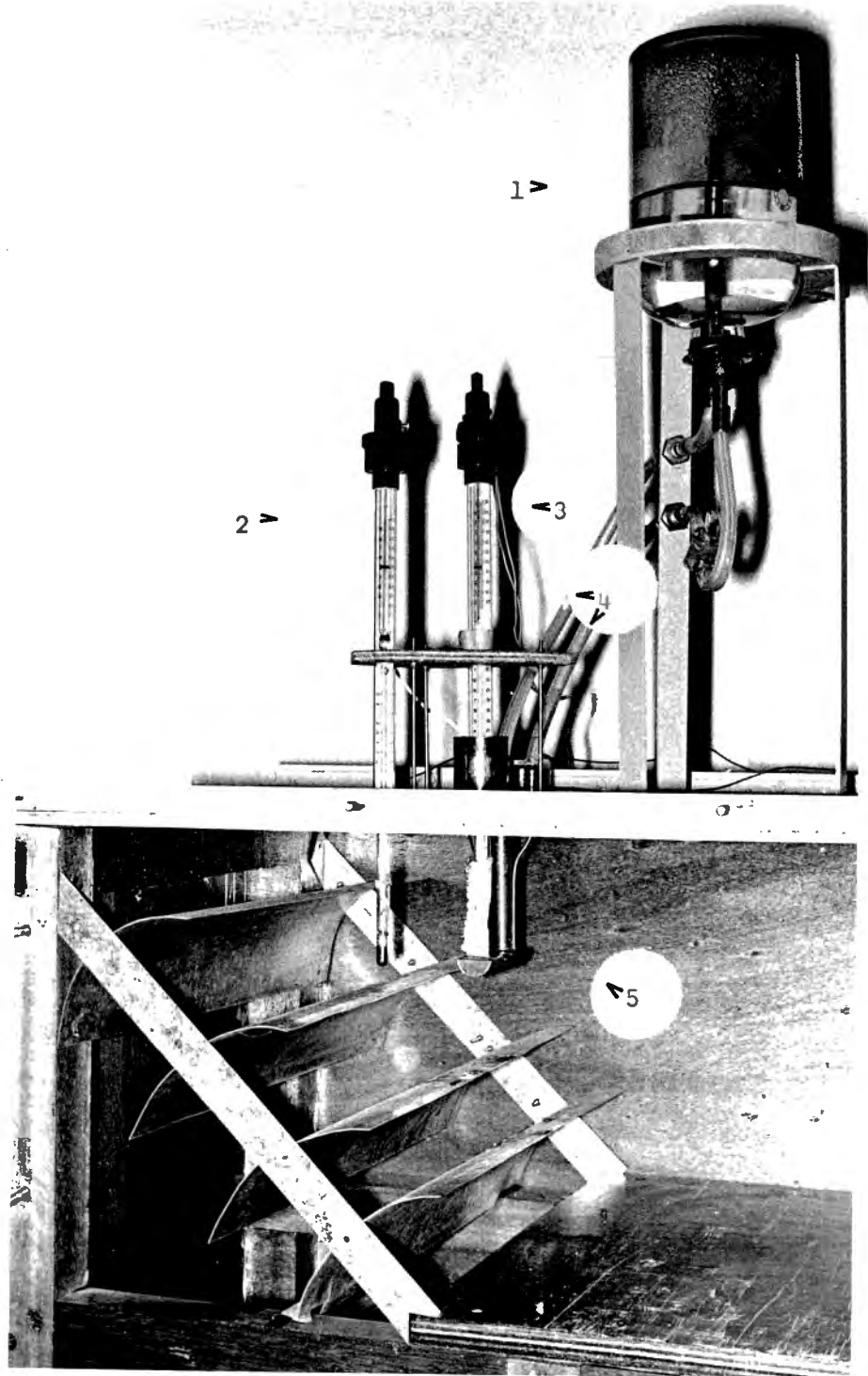


Fig. 6 Wet- and Dry-bulb Temperature Measuring Systems.

1. Distilled water reservoir.
2. Dry-bulb contact thermometer.
3. Wet-bulb contact thermometer.
4. Air pipe and water feed pipe.
5. Copper trough into which dips the muslin sock.

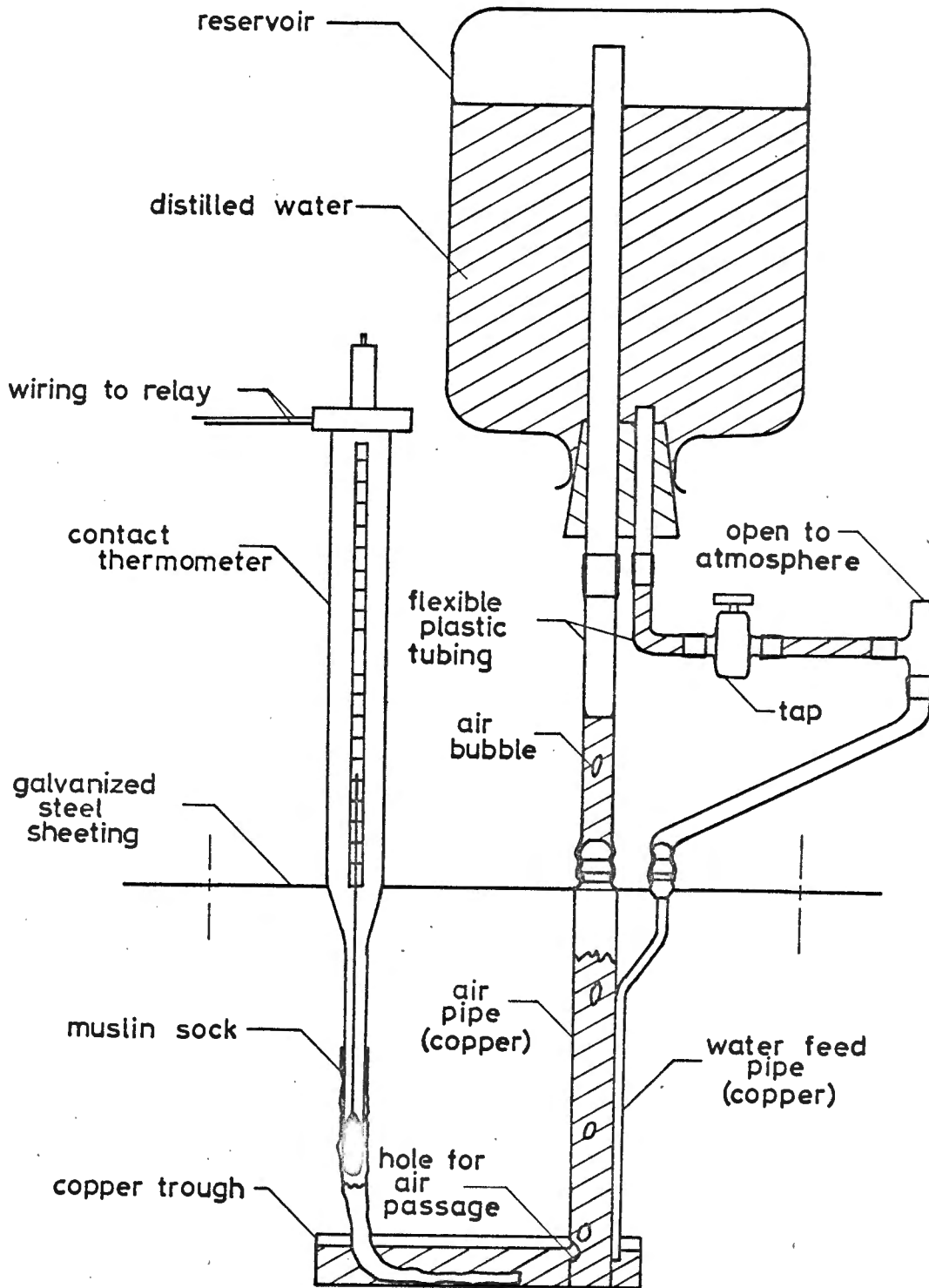


Fig. 7 Wet-Bulb Temperature Measuring System.

recorder was used to record temperatures such as: the dry-bulb temperature before and after the drying section, the wet-bulb temperature, the temperature of 4 apple rings, the water temperature in the water bath, the fan motor temperature and the temperature in the proximity of the electrical resistance heating bars. The temperature sensors were iron-constantan thermocouples, which were coated with a varnish to prevent corrosion which would have resulted in spurious temperature readings.

These temperature recordings were extremely useful in assisting with the control of the wet- and dry-bulb temperature, since from the magnitude of under- or overshoot, the modes of control could be altered accordingly.

3.8 ELECTRICAL SYSTEMS

All electrical switches were mounted on a control panel which was easily accessible to the operator. As a safety procedure, by the switching arrangement, neither the resistance nor the immersion heaters could be switched on without the fan operating.

Since both the wet- and dry-bulb control systems used contact thermometers, the mode of control was on-off. A transformer-rectifying circuit was used to produce 6 volts D.C. from the mains, this voltage was connected across the contact thermometer terminals. Electrical connections of the A.C. circuit are shown in Fig. 8. By means of manual switches, the mode of operation of any heating bar or immersion heater could be set as either permanently on, permanently off, or switched to the on-off control mode of the contact thermometer-relay system.

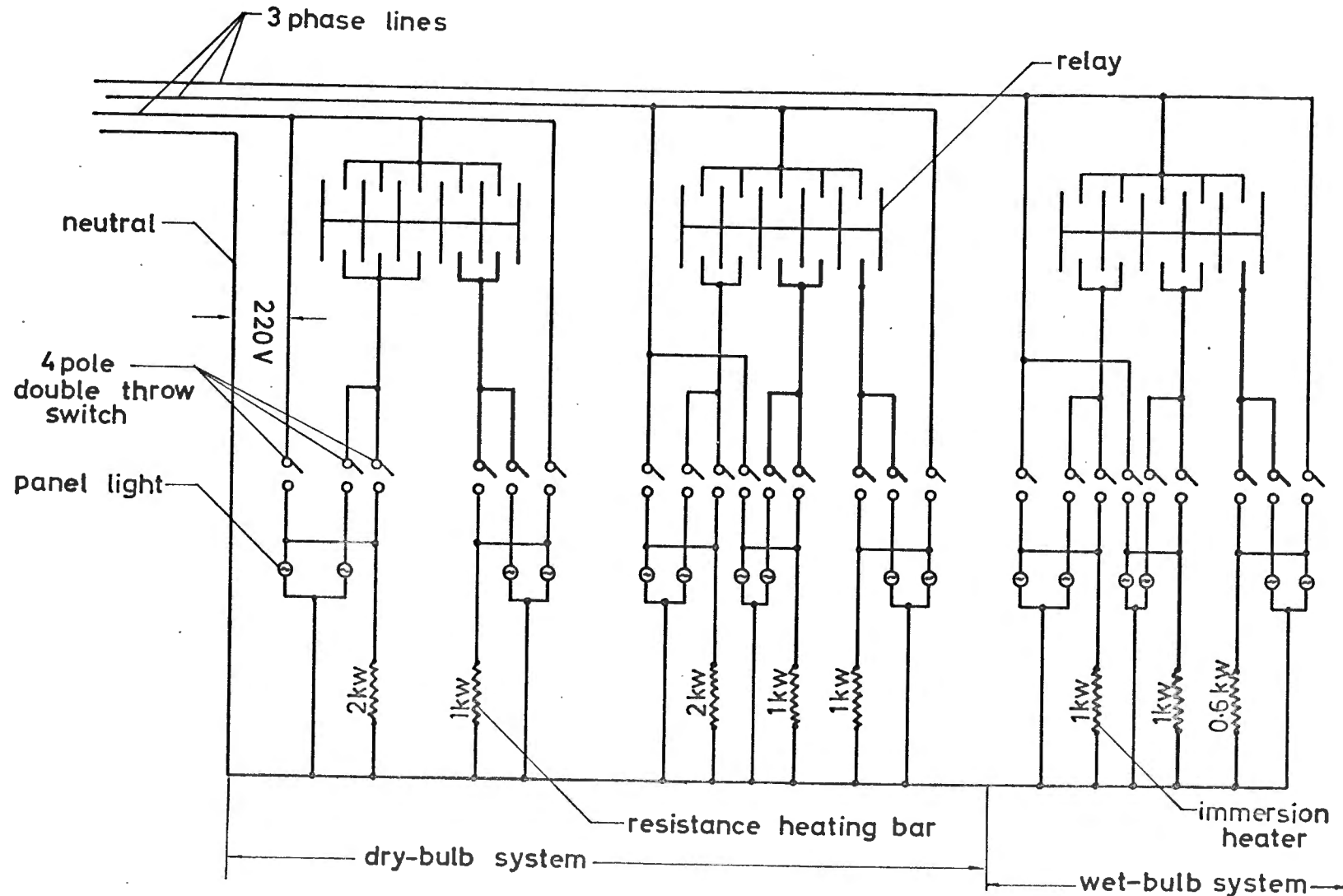


Fig. 8 Circuitry for A.C. Power Input to Wet- and Dry-Bulb Temperature Control Systems

CHAPTER 4.

EXPERIMENTAL PROCEDURE

4.1 INTRODUCTION

The variety of apple used, throughout all experimental work, was the "Granny Smith". The majority of apples had a diameter of between 63 and 75 mm. Those apples not immediately being used for experimental work were stored in cold storage at about 1°C.

It is important to note that in all the work done, the wet-bulb temperature was kept constant. This was practised because the wet-bulb temperature down the length of an industrial dehydrator is virtually invariant, since the system is almost adiabatic. A typical industrial dehydrator wet-bulb temperature of 37.8°C was used.

4.2 PREPARATION OF APPLE RINGS

A very effective apple-peeling and coring machine, shown in Fig. 9, enabled apples to be both peeled and cored within 5 seconds. A spring-loaded blade, which could follow the apple contour, peeled the rotating apple, while a semi-circular blade simultaneously cored it.

Once the apples were peeled and cored, they were sliced to the required thickness with a domestic bread-cutter. The apple rings were then dipped into a 5% solution of sodium metabisulphite for 5 minutes. After this soaking, the apple rings were allowed to drain for 10 minutes to get rid of any excess superficial moisture.

This method of soaking and draining was adhered to in all the work done. Standardization is necessary because the length of soaking and draining determines the amount of water and preservative that is absorbed by the fresh apple rings.

The specifications for sulphur dioxide content, in commercially marketed apple rings, are: not less than 500 ppm in product apple ring or else browning occurs (due to oxidation); not more than 2000 ppm. is permissible [12]. The powerful reducing agent, sulphur dioxide, is evolved from the sodium metabisulphite ($\text{Na}_2\text{S}_2\text{O}_5$) according to the following equations:

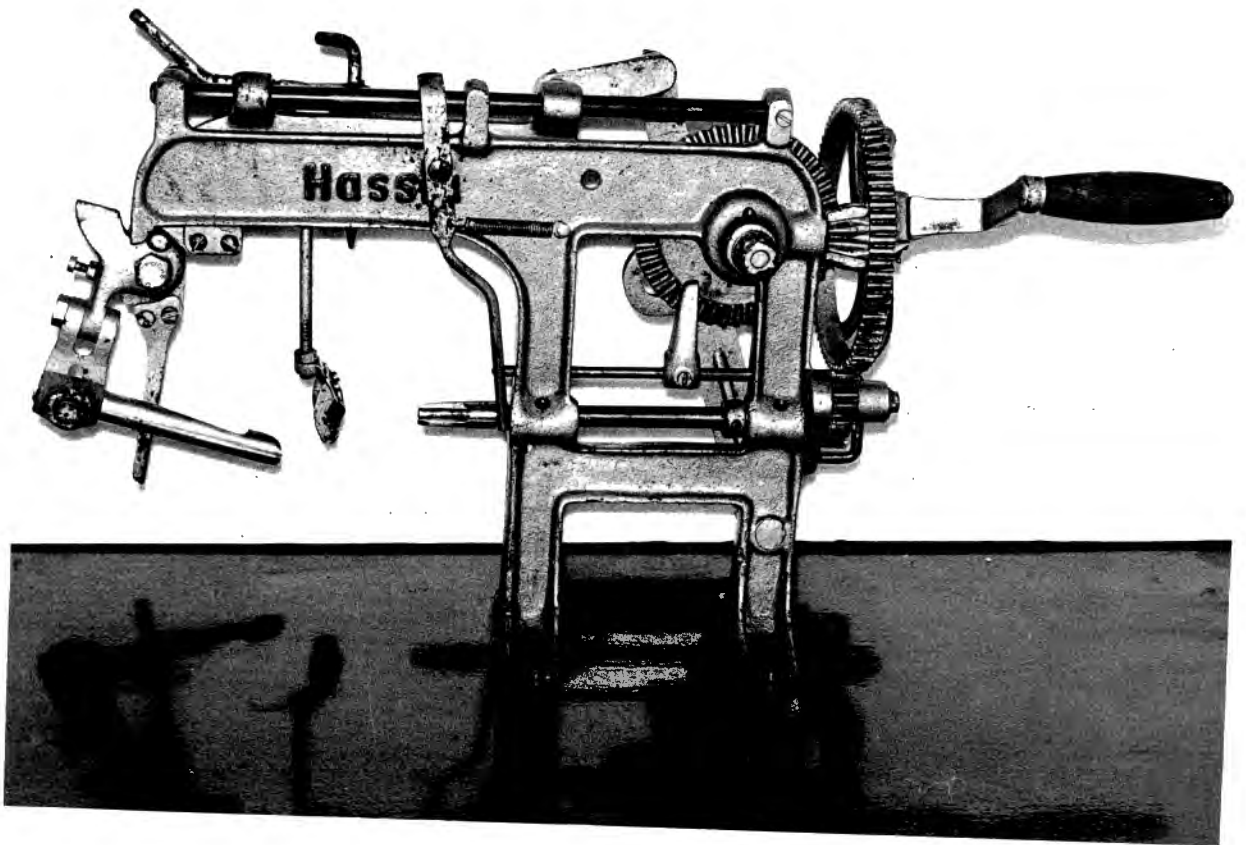
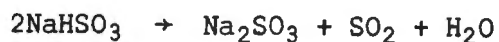
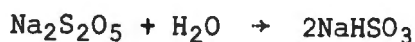


Fig. 9

Apple Peeling and Coring Machine.



After draining, the freshly prepared, moist apple rings were ready for drying. It must be noted that stainless steel apparatus has to be used when cutting and preparing the apples. Iron tends to cause discolouration of the cut fruit. Plastic and wood can also be used without causing discolouration.

4.3 GENERAL OPERATIONAL PROCEDURE OF THE WIND-TUNNEL

The required wet- and dry-bulb temperatures were set on the two contact thermometers. Tap water was allowed to run into the constant head reservoir that supplied the immersion heater water-bath. The fan and control systems were then switched on and allowed to run until the circulating air had acquired the correct humidity and temperature. During this period the apple rings were prepared.

As soon as the wet- and dry-bulb control systems were controlling about their set points, the air velocity was measured and set at the desired value. The fan was then switched off and the apple rings either spread on the tray (gaining accessibility to the tray through the door of the drying section), or the whole drying section cartridge, previously loaded with apple rings, was inserted into the drying section. The packed length and width of the apple rings, on the tray, was noted. The fan and control systems were simultaneously switched on. At pre-determined intervals, the fan was switched off and the weight readings noted. It was necessary to switch the fan off during weight readings in order to avoid the effect of drag, exerted by the circulating air, on the tray and contents. The complete weighing procedure, from switching the fan off to switching it on again, took a maximum time of 20 seconds.

At the conclusion of the run the apple rings were removed from the tunnel and analysed for moisture content.

4.4 EQUILIBRIUM CURVE

In equilibrium moisture content determinations, the apple rings

were allowed to dry under constant external conditions of temperature and humidity, until no further weight loss was noted. The apple rings had thus equilibrated with their environment and analysis of the rings yielded the equilibrium moisture content, under those specific environmental conditions. In this fashion, by performing a series of experimental runs over a range of humidities, the equilibrium moisture content curve of apple rings was found.

4.5 DRYING RATE CURVES

The apple rings were dried under constant external conditions of air velocity, humidity and temperature. Sixteen apple rings, packed on the tray, with a configuration as shown in Fig. 10, were used for each drying rate curve. The area occupied by the rings on the tray, as well as the initial load of apple rings, was noted prior to the commencement of the run.

To observe the evaporative cooling effect of the moisture leaving the apple rings, four thermocouples were inserted into the apple rings and their temperatures recorded continuously on the multi-point temperature recorder.

In a number of rate determination runs done, apple rings were dried to equilibrium, thus yielding additional data for the equilibrium moisture content curve.

Initially, it had been hoped that point-condition drying rate curves would be measured, by virtue of the fact that mixing of the air, passing over the apple rings, would be sufficient for the temperature differential across the tray load to be minimal. At higher drying rates a temperature differential was found to exist between the inlet and outlet of the tray. This was significant enough to cast doubt upon an assumption of point drying conditions. Experimental work was done to show the effect of packed length of apple rings on the drying rate - half of the usual packed length was used in this investigation. In effect, drying rate curves, obtained in this work, give a mean drying rate for a packed length of 230 mm.

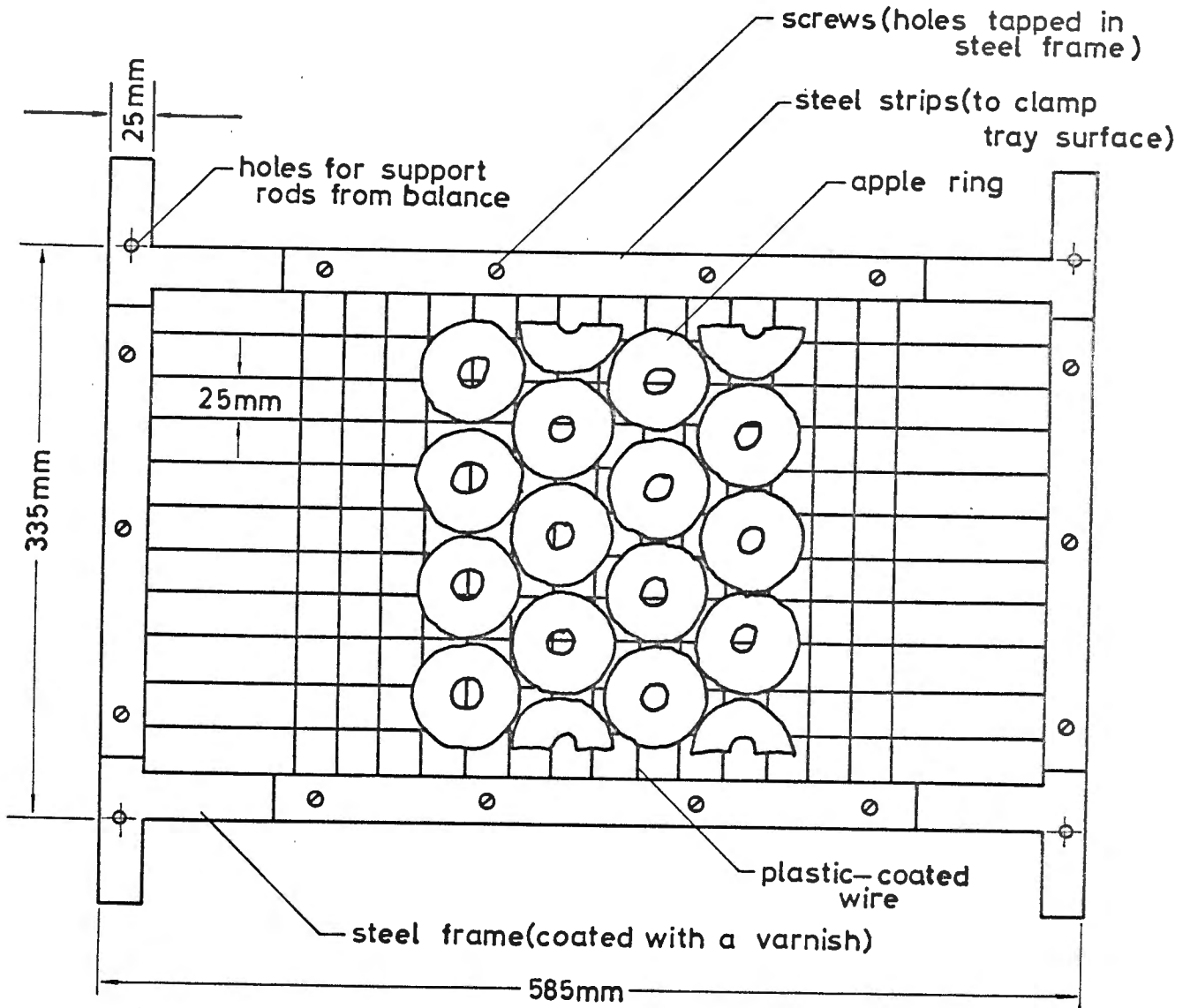


Fig. 10 Layout of Apple Rings packed on the Tray for drying under Constant External Conditions.

4.6 SIMULATION RUNS

These experimental runs were performed in order to simulate the drying conditions which prevail in a typical parallel-flow industrial dehydrator.

The industrial dehydrator that was simulated had 10 trucks in the tunnel, therefore, since these tunnels operate in a quasi-continuous fashion, each truck remains in a specific position in the tunnel for one tenth of the total drying time.

The three plastic-coated wire trays, discussed in section 3.4, were completely covered with a single layer of apple rings. These rings were packed in an analogous way to that used in drying rate determinations. A tray spacing, similar to that used in the industrial situation, was chosen and the trays arranged accordingly.

A realistic total drying time was chosen for the simulation runs. In these runs, the input dry-bulb temperature to each simulated tray position was given by the output dry-bulk temperature from the previously simulated tray position. These output temperatures, from any simulated tray position, varied with time due to the drying characteristics of the apple rings. Therefore, when these output temperatures were used as the input to the next simulated position; the set-point of the dry-bulb contact thermometer was adjusted with time. For the initial simulated drying position, the input temperature was held constant.

In this manner, each of the ten tray positions in the industrial dehydrator were simulated and, finally, the apple rings were analysed for total moisture content. Representative samples of the dried apple rings were taken, yielding an average moisture content. Generally, the moisture distribution down the length of the tray was insignificant, therefore an average moisture content for the whole tray was meaningful.

In the initial simulation runs, spurious output temperature readings from the tray (provided by the thermocouple-multipoint recorder system) were obtained, because a temperature profile existed in the space between any two of the three trays. This was particularly

noticeable at high drying rates. This difficulty was remedied by placing a mixing box (consisting of a rectangular conduit, with a doughnut-ring type constriction, which forced the air to mix prior to measurement) directly after the tray outlet which thus enabled the measurement of an average temperature, rather than a point temperature.

4.7 MOISTURE CONTENT ANALYSIS

The moisture content of the apple rings was found by vacuum oven analysis. The samples were placed in the vacuum oven and the air exhausted from the oven using a high vacuum pump. To ensure that the air, used to sweep out the oven, was dry and clean it was passed through a tube of anhydrous calcium chloride and then bubbled through concentrated sulphuric acid before it entered the oven.

The usual method used for analysing apple rings is as follows [13]: "Sample ground in food chopper, Hobart mixer, or blender. Drying 6 hours at 70°C, oven pressure not over 100 mm. mercury. A.O.A.C.(1960)".

The method of vacuum drying adopted in this work deviated from the above procedure. For all experimental runs performed, three analyses were done on the product apple rings. A representative sample of the apple rings to be analysed was taken, and each ring divided into three equal segments. Thus three samples, comprising of one segment from each apple ring, were available for analysis. The apple ring samples were dried for 10 hours at 70 mm. mercury pressure and at 70°C. An air-sweep of about 1cc per second was used. It was found that drying for a shorter period was unsatisfactory since the samples were not completely dry.

The moisture content of the apple rings was calculated on a difference basis by noting the weight of each sample prior to vacuum drying W , and the weight of the bone-dry apple after vacuum drying, D . Eqn. shows how the total moisture content, X_T , may be calculated:

$$X_T = \frac{W-D}{D} \quad (11)$$

It was found impracticable to vacuum-dry fresh fruit and dried rings simultaneously, since, invariably the vapour pressure

exerted by the moisture in the fresh fruit was sufficiently high to cause the dried rings to absorb water from the oven environment.

A typical moisture content calculation is given in Appendix B.

CHAPTER 5

RESULTS.

5.1 INTRODUCTION

The results of this investigation may be classified into 3 main sections, namely: the equilibrium curve determination, the evaluation of the drying rates under constant external conditions and the experimental simulation of an industrial dehydrator. The drying rate curves obtained under constant external conditions, are subsequently used in the computational simulation of drying in a typical industrial dehydrator.

5.2 EQUILIBRIUM CURVE

The equilibrium moisture content curve for apple rings, equilibrated at a constant wet-bulb temperature of 37.8°C, is shown in Fig. 11, where the equilibrium moisture content, X_T^* , is plotted against the percentage relative humidity of the air, Hr^* . The shape of this curve is characteristic of the equilibrium curves of hygroscopic solids, where at elevated humidities the solid contains a fairly high amount of water, while at the lower range of humidity the equilibrium moisture content is low.

This curve may be described by an equation of the form:

$$X_T^* = \frac{e Hr^* + f Hr^{*2}}{1 + g Hr^*} \quad (12)$$

The curve resulting from Eqn. (12) passes through the origin, and, in addition, it was constrained to pass through the value of the total moisture content of the freshly prepared apple rings, at an absicca value of 100 percent relative humidity. For subsequent calculation purposes, the coefficients e, f and g in Eqn. (12), were determined (by least squares criteria) and are:

$$\begin{aligned} e &= 0.002118 \\ f &= -0.00001634 \\ g &= -0.0099289 \end{aligned}$$

At the same time, Hr^* and X_T^* may be correlated by:

$$Hr^* = \frac{356.06X_T^* + 5494.7X_T^{*2}}{1 + 6.1236X_T^* + 54.437X_T^{*2}} \quad (13)$$

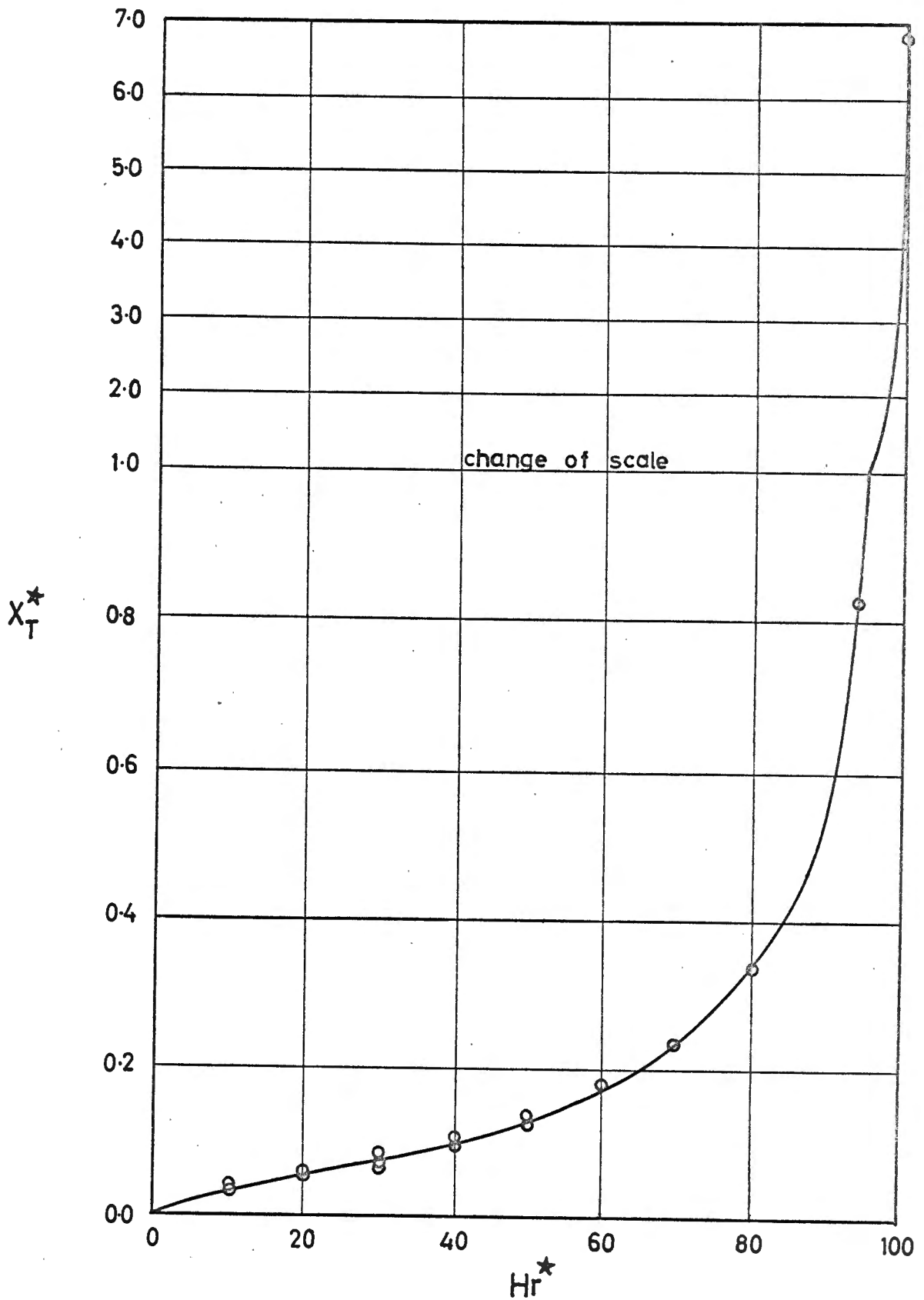


Fig. 11 Equilibrium Moisture Content Curve of 6.4 mm Thick Apple Ring Slices

Eqn. (13) gives the percentage relative humidity of the air with which the apple rings would have to equilibrate to result in an equilibrium moisture content of X_T^* . Thus Eqns. (12) and (13) may now be used in drying calculations, requiring a knowledge of the equilibrium moisture content, X_T^* , or the equilibrium percentage relative humidity of the air, Hr^* .

Equilibrium data is tabulated in Appendix A.

5.3 DRYING UNDER CONSTANT EXTERNAL CONDITIONS

In an endeavour to describe the drying of apple rings on a quantitative basis, drying rate curves were obtained under different controlled external conditions.

For each experimental run performed, a drying curve of apple load versus time is obtained. A typical curve of total moisture content, X_T , versus time is given in Fig. 12. The value of X_T at any time (during drying) may be calculated from the weight of the load on the tray, W_2 , and the total bone-dry weight of the apple load, D_1 :

$$X_T = \frac{W_2 - D_1}{D_1} \quad (14)$$

To evaluate D_1 it was necessary to know the final weight of the product apple rings on the tray, W_1 , and their total moisture content, X_{T_1} (found by vacuum analysis).

$$D_1 = \frac{W_1}{1 + X_{T_1}} \quad (15)$$

Sample calculations, of X_T and D_1 , are given in Appendix B.

Eqn. (14) may be used to calculate the total moisture content of the freshly prepared apple rings, by substituting into it the weight of the initial tray load. At the same time, the moisture content of the freshly prepared apple rings may also be obtained from vacuum oven analyses, so that this provides a suitable check on accuracy. Table 1 compares the values of total moisture content found by these 2 methods; agreement is within the limits of

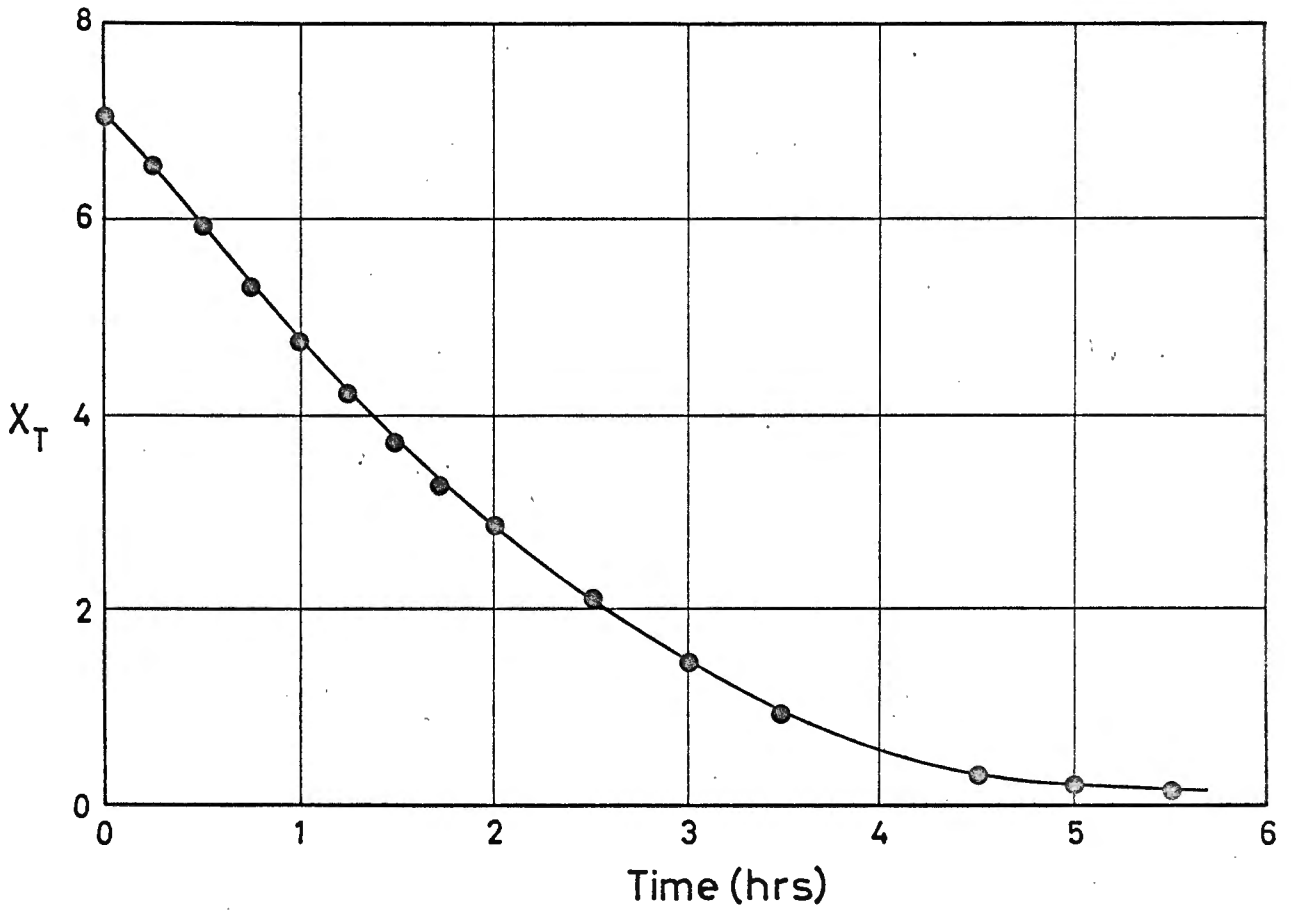


Fig. 12 Drying Curve of 6.4 mm Thick Apple Ring Slices at 40
Percent Relative Humidity.

● Run No. 3

experimental error, which indicates that application of Eqns. (14) and (15) yields satisfactory results.

X_T , COMPUTED	X_T , ANALYSIS
6.779	6.530
7.099	7.210
6.684	6.402
6.337	6.541
6.8953	6.628

TABLE 1 Comparison of some values, of total moisture content of freshly prepared apple rings, obtained by computational and by analytical means.

Drying rates were computed by fitting a second order polynomial to 5 consecutive data points (of load weight per unit area versus time), using the least squares criteria to give the best fit. The rate at the central data point was then given by the slope of the fitted curve at that point.

Rate curves were determined, to evaluate the effect of the following factors on drying rates: humidity, apple ring thickness, tray surface and air velocity. Work was also done to show constant-rate drying, and the effect of packed apple length on an assumption of point drying conditions.

Rate results are tabulated in Appendix C and are discussed in later sections and a sample calculation of drying rate is also given in Appendix C.

5.4 THE INFLUENCE OF HUMIDITY ON DRYING RATES

The relative humidity of the drying air, H_r , is the most important single factor in drying [14], since the lower the air humidity, the larger is the driving force. Furthermore, the higher the dry-bulb temperature, the more favourable is the driving force,

since the saturation vapour pressure of water, p_s , increases with temperature. Eqn. (5) illustrates these 2 points:

$$D.F. = 0.01(Hr^* - Hr)ps \quad (5)$$

A number of drying rate curves for 6.4 mm thick apple slices, obtained at a constant wet-bulb temperature of 37.8°C and variable dry-bulb temperatures, are shown in Fig. 13. In these experimental runs the air mass velocity was kept approximately constant. The open, plastic-coated, wire tray was used in these experimental runs.

The curves, in Fig. 13, are a plot of the drying rate (in g H₂O/m²sec.) versus the free moisture content of the apple rings, X , which is calculated from Eqn. (1):

$$X = X_T - X_T^* \quad (1)$$

It would be desirable to be able to express the numerous curves, shown in Fig 13, in terms of a single curve. This was achieved by normalizing the drying rates, according to the procedure discussed in section 2.4, by applying Eqn. (10):

$$\frac{\frac{dw}{dt}}{[0.01(Hr^* - Hr)ps]^B} = A X_T^C \quad (10)$$

or

$$\frac{\frac{dw}{dt}}{(D.F.)^B} = A X_T^C \quad (16)$$

The term on the left of Eqn. (16) may be called the "specific rate". The coefficients A, B and C were evaluated by a least squares matrix solution, using the data for 6.4 mm rings, given in Fig. 12 as well as data from section 5.8. The resultant values of the coefficients A, B and C are:

$$\begin{aligned} A &= 0.01206 \\ B &= 0.60688 \\ C &= 0.56170 \end{aligned}$$

Both the normalized data, and the curve described by Eqn.(10) are shown in Fig. 14. The data points (for relative humidities between 10 and 40 percent) mostly lie close to the curve and therefore

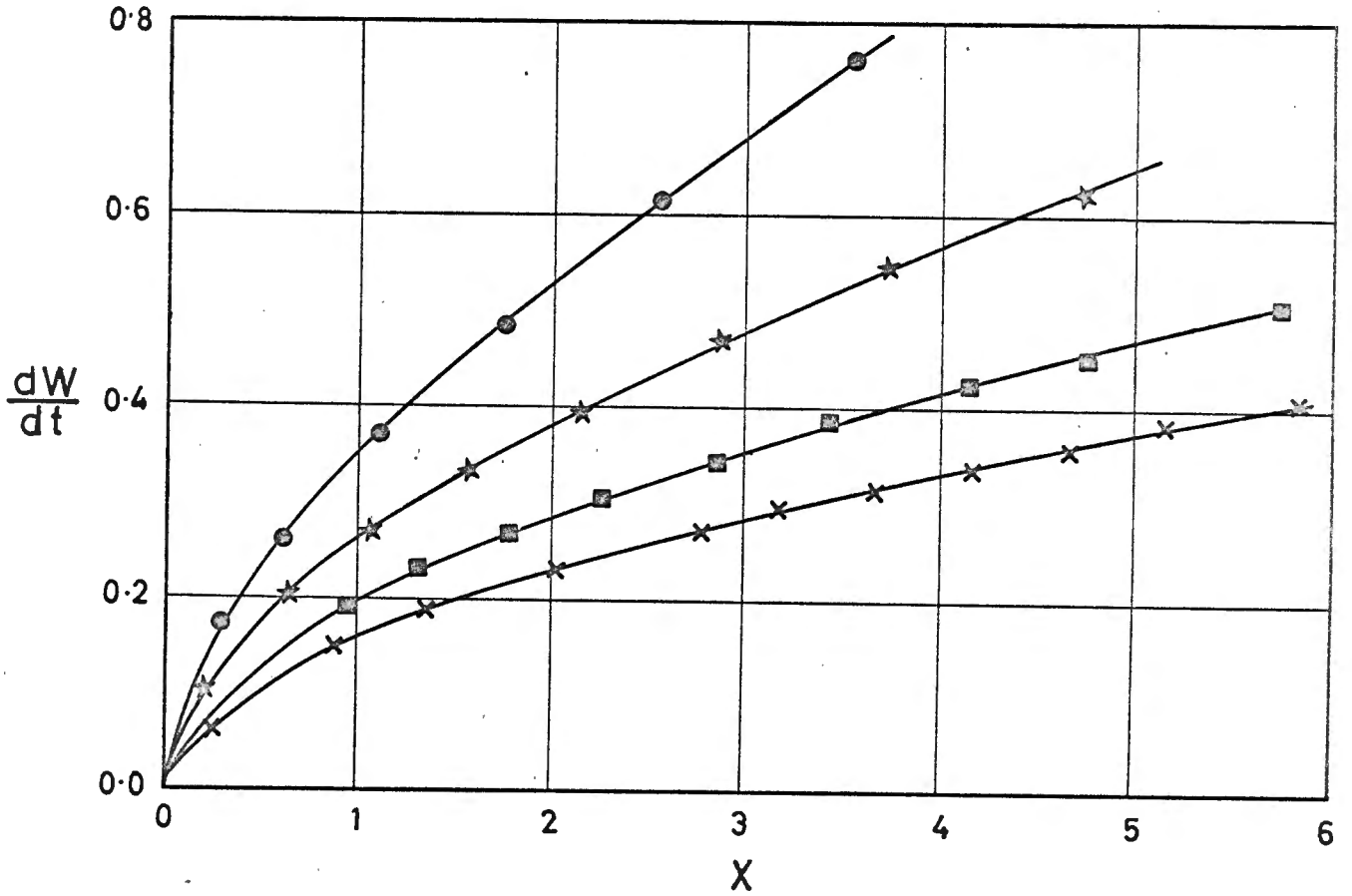


Fig. 13 The Effect of Humidity on the Drying Rate of 6.4 mm Thick Apple Ring Slices

<u>percentage relative humidity</u>		<u>Run No.</u>
●	10	1
★	20	2
■	30	5
×	40	3

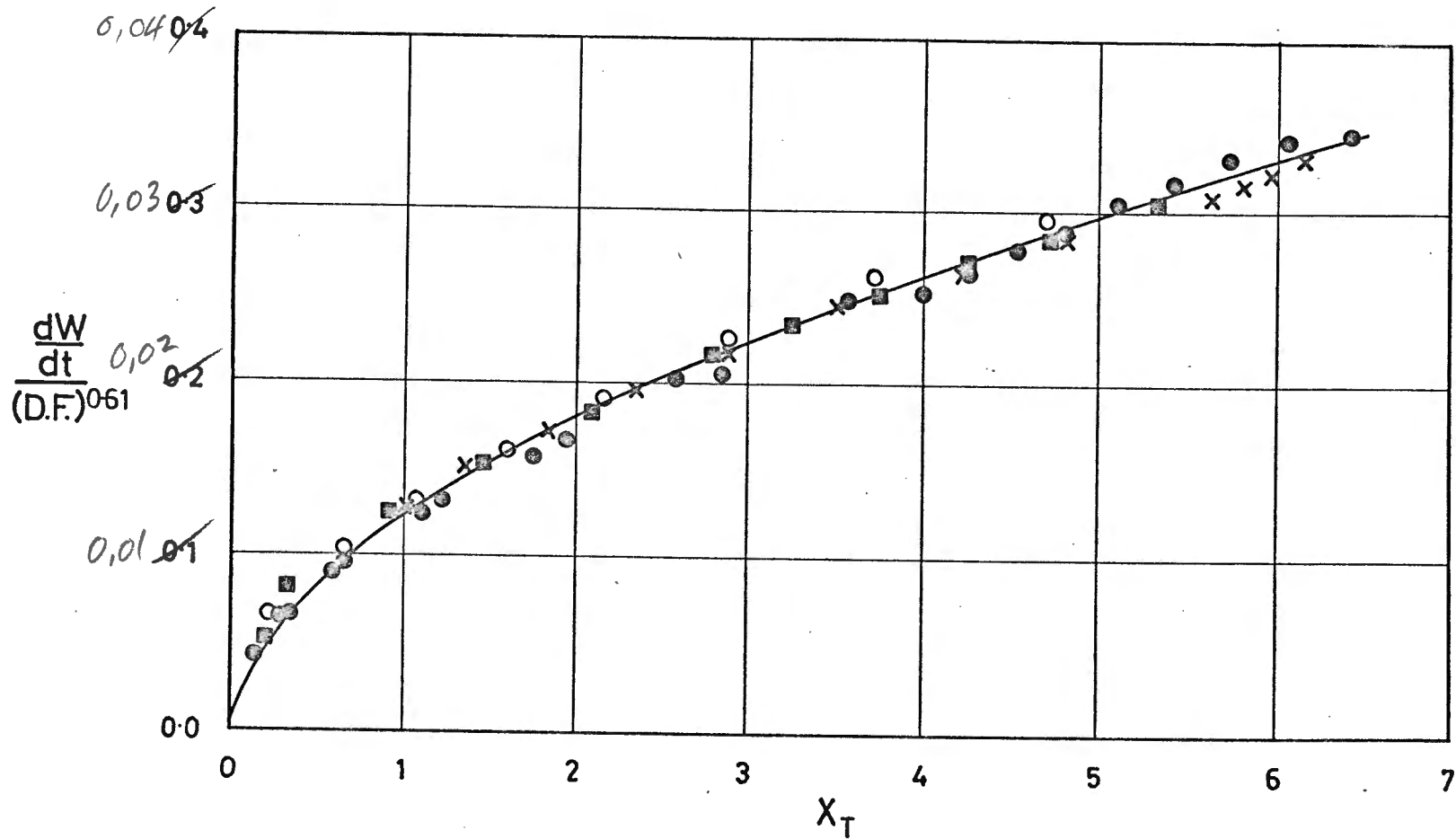


Fig. 14 Normalized Drying Rate Curve for 6.4 mm Thick Apple Ring Slices - Eqn.(10)

	<u>Percentage relative humidity</u>	<u>Run Nos.</u>
●	10	1,4
○	20	2
×	30	5
■	40	3

Eqn. (10) appears to be general enough to use for predicting drying rates in and about the 10 to 40 percent relative humidity range.

The values of Hr^* , used to normalize the data, were calculated from the total moisture content, X_T , as follows:

$$Hr^* = \frac{356.06X_T^* + 5494.7X_T^{*2}}{1 + 6.1236X_T^* + 54.437X_T^{*2}} \quad (13)$$

5.5 THE EFFECT OF APPLE THICKNESS ON DRYING RATES

A number of rate curves measured at 20 and 40 percent relative humidity, using the plastic-coated wire tray, are shown in Figs. 15 and 16 respectively. The different apple ring thickness for which these curves were obtained, were: 3.2, 6.4, 7.9 and 9.5 mm. These results were obtained using approximately the same air mass velocity.

These rate curves show that the drying rate at any value of the free moisture content, X , decreases with an increase in apple ring thickness. However, the curves appear to "saturate" as the ring thickness increases and the effect of thickness on the drying rate becomes less marked; the difference between the drying rates of 7.9 and 9.5 mm slices is small.

TABLE 2
Coefficients
for Eqn. (10)

Slice thickness in mm.	A	B	C
3.2	0.01100	0.67952	0.46342
6.4	0.01206	0.60688	0.56170
7.9	0.00669	0.72004	0.59888
9.5	0.00646	0.71231	0.63499

The results obtained for the 3.2, 7.9 and 9.5 mm slices were also normalized in an analogous fashion to those for the 6.4 mm slices, as discussed in section 5.4. Each set of results, for the different thicknesses, yielded corresponding values of the coefficients A, B and C for Eqn. (10). The values of these coefficients, as well as those found for the 6.4 mm slices, are given in Table 2.

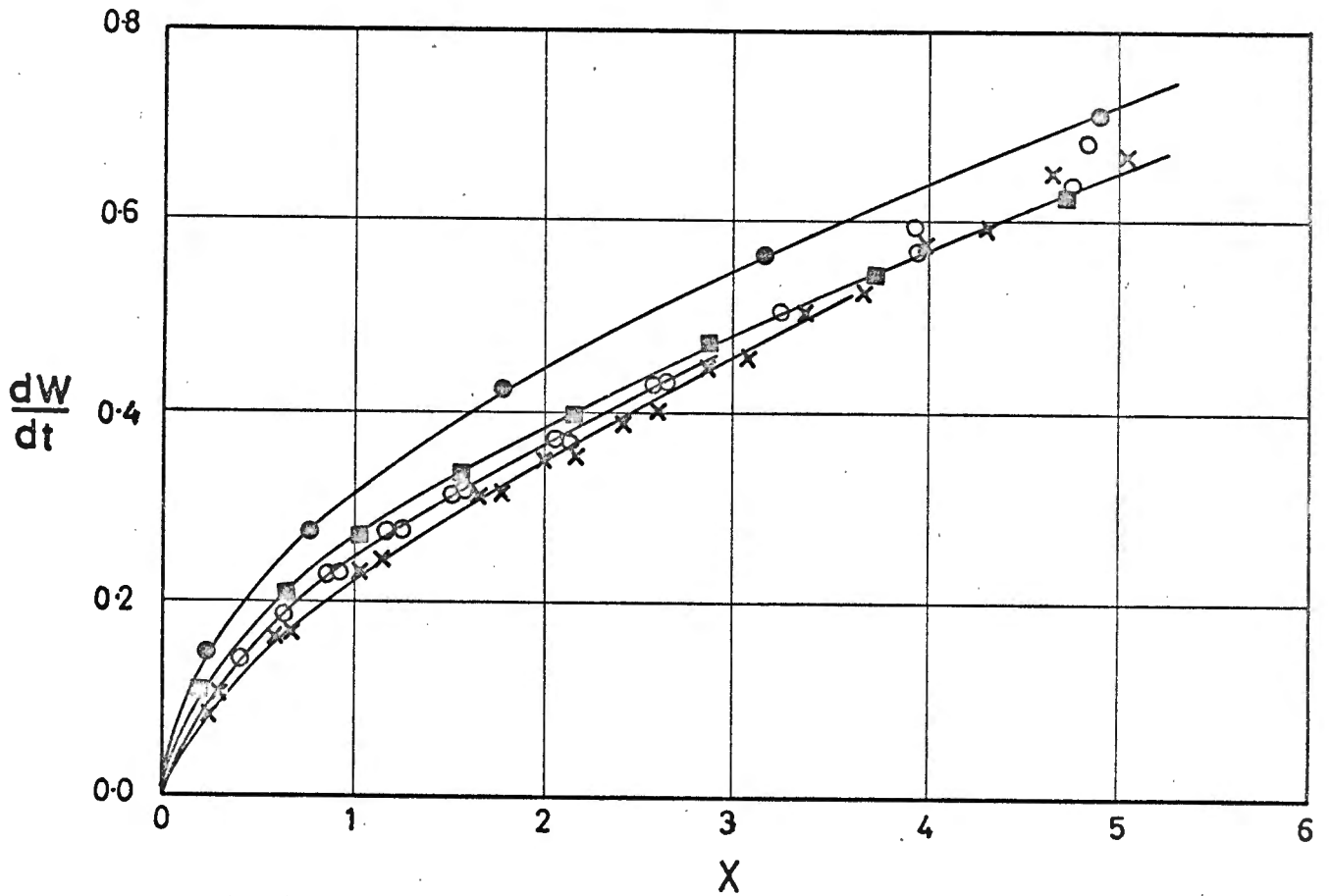


Fig. 15 The Effect of Apple Ring Slice Thickness on Drying Rates at 20 Percent Relative Humidity.

	<u>Thickness</u>	<u>Run Nos.</u>
●	3.2 mm	14
■	6.4 mm	2
○	7.9 mm	6,7
×	9.5 mm	12,13

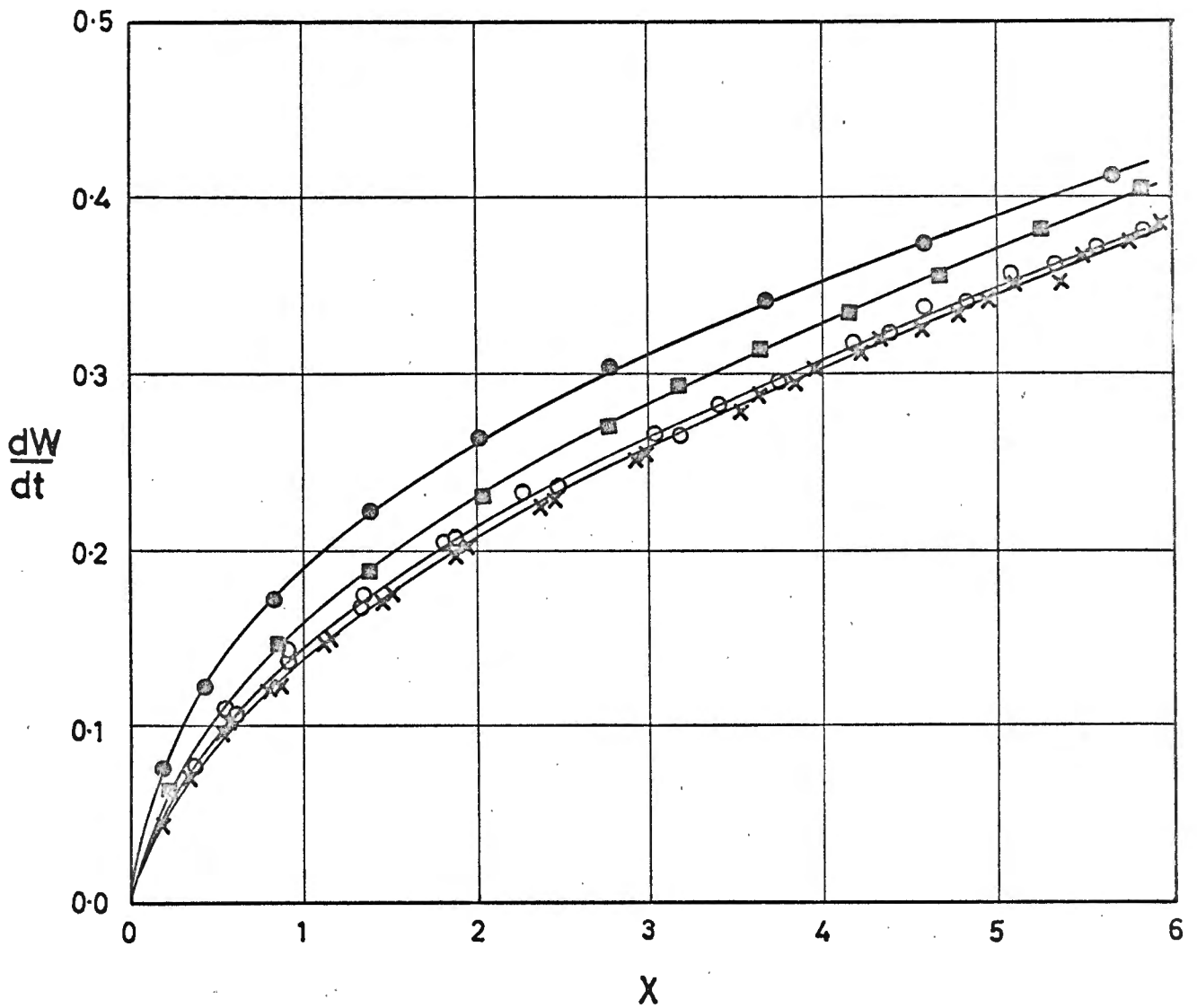


Fig. 16 The Effect of Apple Ring Slice Thickness on Drying Rates at 20 Percent Relative Humidity

	<u>Thickness</u>	<u>Run Nos.</u>
●	3.2 mm	15
■	6.4 mm	3
○	7.9 mm	8,9
×	9.5 mm	10,11

5.6 COMPARISON OF SOLID AND OPEN TRAY SURFACES

Apple rings, with a thickness of 6.4 mm, were dried at 40 and 20 percent relative humidity on the solid tray. The resultant drying rate curves are shown in Figs. 17 and 18, together with the curves found under similar conditions on the open, plastic-coated, wire tray.

In addition, the ratio of the drying rates obtained using the two different trays, is given in Fig. 19 for the two conditions of humidity. These curves illustrate how much of a detrimental effect a solid surface has on drying rates. This is explicable since, with the solid tray, only about half of the potential drying surface is exposed for drying, as compared with the wire-tray. Also, in the solid surface situation, moisture has to diffuse from the surface in contact with the tray, through to the surface exposed to the air. Since the major resistance to mass transfer lies in the diffusional resistance, this is another factor which curtails the rate of drying from a tray of this nature.

Because the resistance to mass transfer in an apple ring may be assumed to be proportional to a power of the drying rate (discussed in section 2.5), this probably explains why the rates, on the solid surface, at 20 percent relative humidity are affected to a larger extent than those at 40 percent. The moisture has to diffuse through a greater thickness of apple (in the solid surface situation), thus at high rates the resistance increases markedly.

A phenomena noticed, with regards the apple ring temperatures, was that for drying on the solid surface, the temperatures were invariably higher than those measured while drying on the open tray. This was particularly noticeable when the fruit still had a high moisture content, i.e., in the vicinity of the wet-bulb temperature. It is felt that these higher temperatures were a result of heat being conducted through the solid tray, from the underside, to the apple rings.

5.7 EFFECT OF VELOCITY ON DRYING RATES

Air velocities between about 240 and 120 m/min. were used

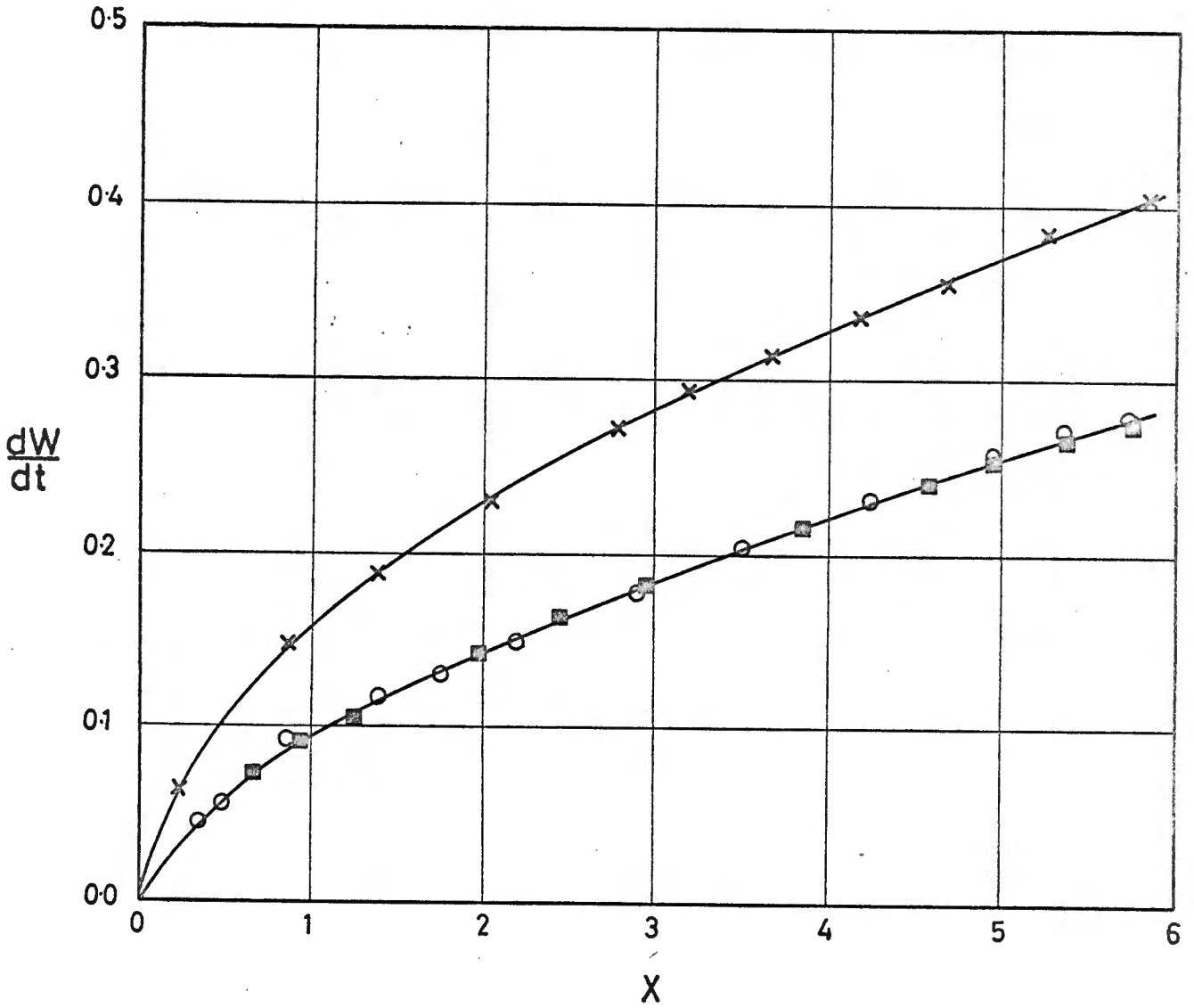


Fig. 17 The Effect of Tray Surface on Drying Rates of 6.4 mm Thick Apple Ring Slices at 40 Percent Relative Humidity.

	Run Nos.
x plastic-coated, wire tray surface	3
■ solid tray surface	16
○ solid tray surface	17

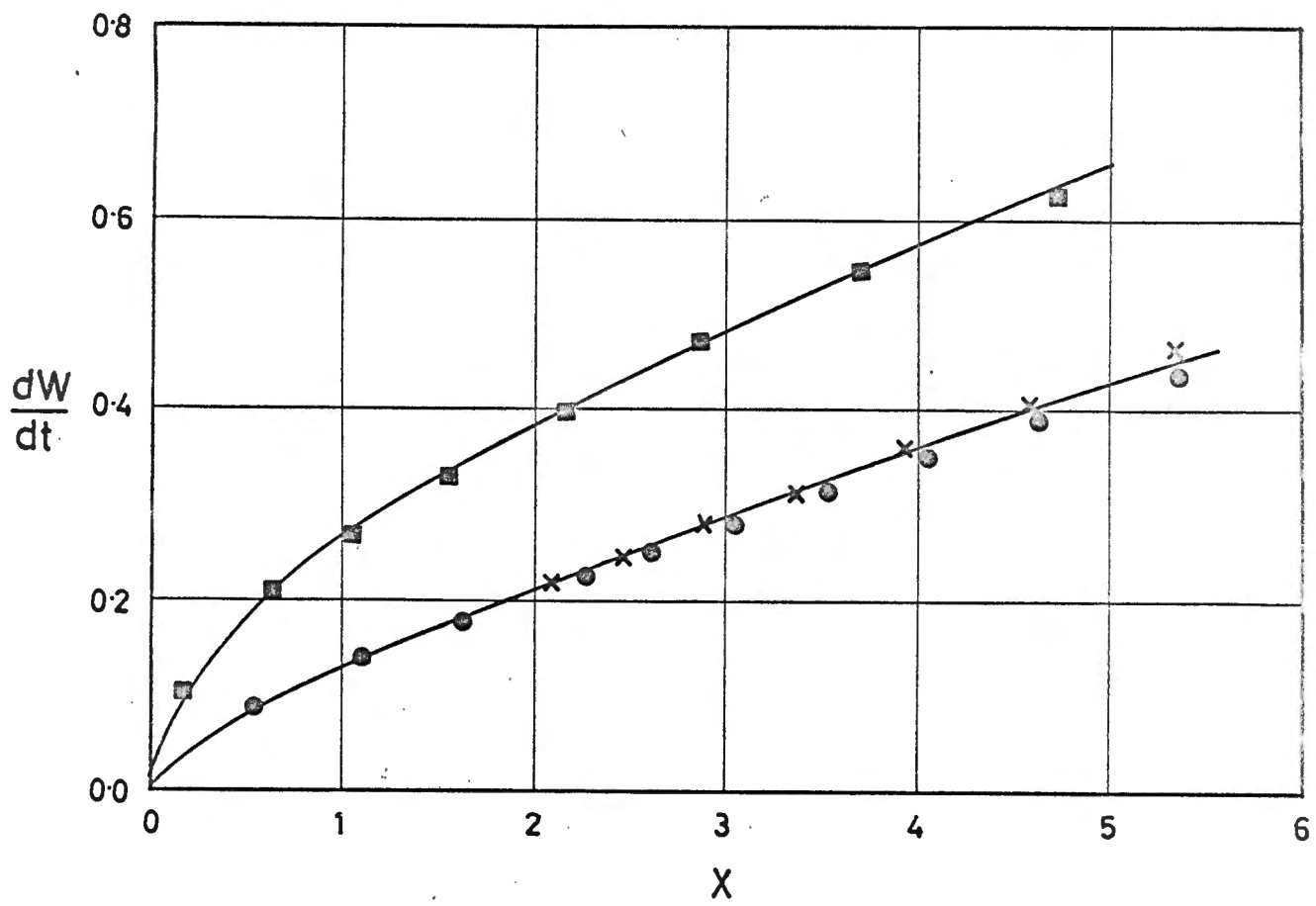


Fig.18 The Effect of Tray Surface on Drying Rates of 6.4 mm Thick Apple Ring Slices at 20 Percent Relative Humidity.

- plastic-coated, wire tray surface Run No. 2
- × solid tray surface Run No. 19
- solid tray surface Run No. 18

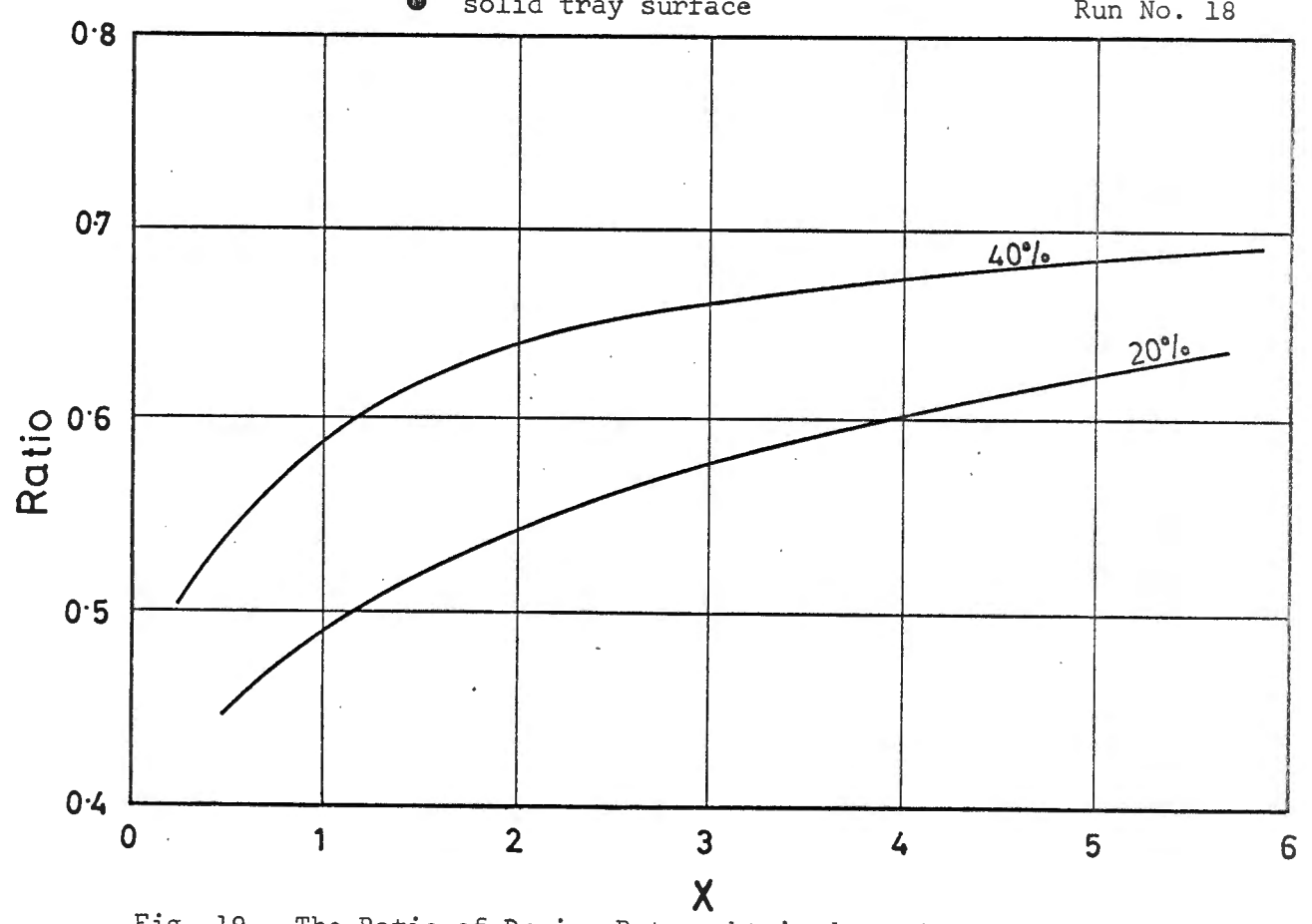


Fig. 19 The Ratio of Drying Rates obtained on the Solid Tray Surface to those on the Plastic-Coated, Wire Tray Surface (for 20 and 40 Percent Relative Humidity).

to dry 6.4 mm. thick apple slices, on the plastic-coated, wire tray. The rate results, shown in Figs. 20 and 21, for drying at 20 and 40 percent relative humidity respectively, illustrate how drying rates decrease with the air velocity.

The rate of evaporation from a free water surface is proportional to the power of 0.8 of the air velocity across the surface [15]. Guillou found that the drying rate of prunes increases only as a power of 0.2 of the air velocity [16]. From the results obtained in this work, the drying rate of 6.4 mm. thick is approximately proportional to a power of 0.5 of the air velocity.

5.8 CONSTANT-RATE DRYING

In initial experimental work, the first experimental readings were taken after the apple rings had dried for a period of 15 minutes. This interval of time was sufficiently long to exclude measurements of drying rates in a region where constant-rate drying was possible. Further experimental runs were performed in which the initial drying rates were included, by initially taking weight readings every 3 minutes. Fig. 22 shows the resultant rate curves obtained for 6.4 mm. thick apple slices, dried on the wire tray, at different air velocities and humidities.

From Fig. 22 it may be seen that there is no region on any of the rate curves where rates remain constant for any extended value of free moisture content, X . In fact, for the 10 percent relative humidity case, drying rates decrease immediately on drying.

This absence of a well defined region of constant-rate drying is possibly a result of drying characteristics exhibited by a typical hygroscopic material, or may be due to poor control of the dry- or wet-bulb temperature at the start-up of the experimental runs.

5.9 INVESTIGATION INTO THE EFFECT OF FINITE PACKED LENGTH OF APPLE RINGS ON AN ASSUMPTION OF POINT-DRYING CONDITIONS.

To determine the effect of the finite packed length of apple rings on assumption of point-drying conditions, a length of about 115 mm. of apple rings was used in experimental runs. This was about

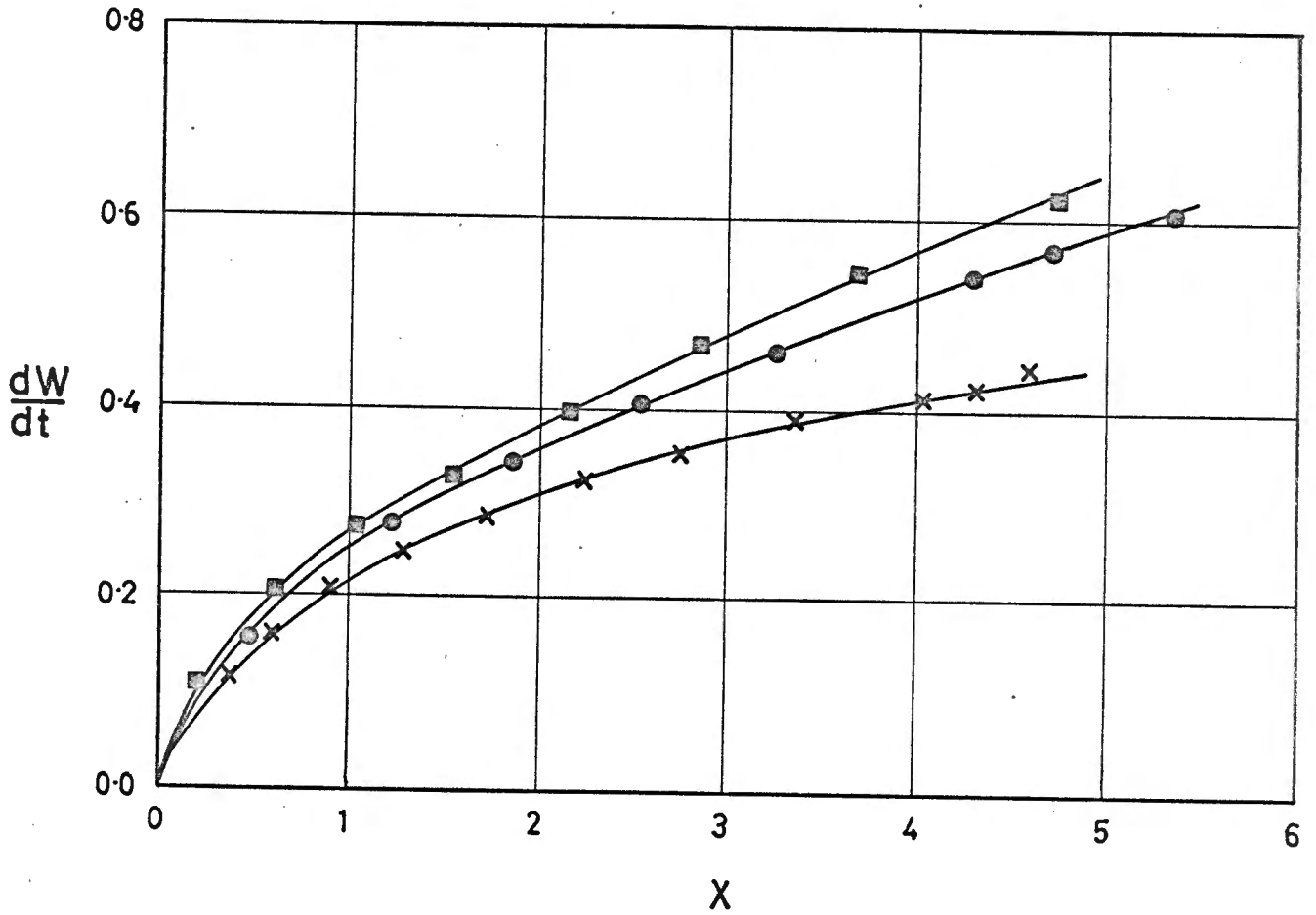


Fig. 20 The Effect of Air Velocity on the Drying Rates of 6.4 mm Apple Ring Slices at 20 Percent Relative Humidity.

	<u>Air Velocity</u>	<u>Run Nos.</u>
■	238 m/min	2
●	183 m/min	20
×	122 m/min	22

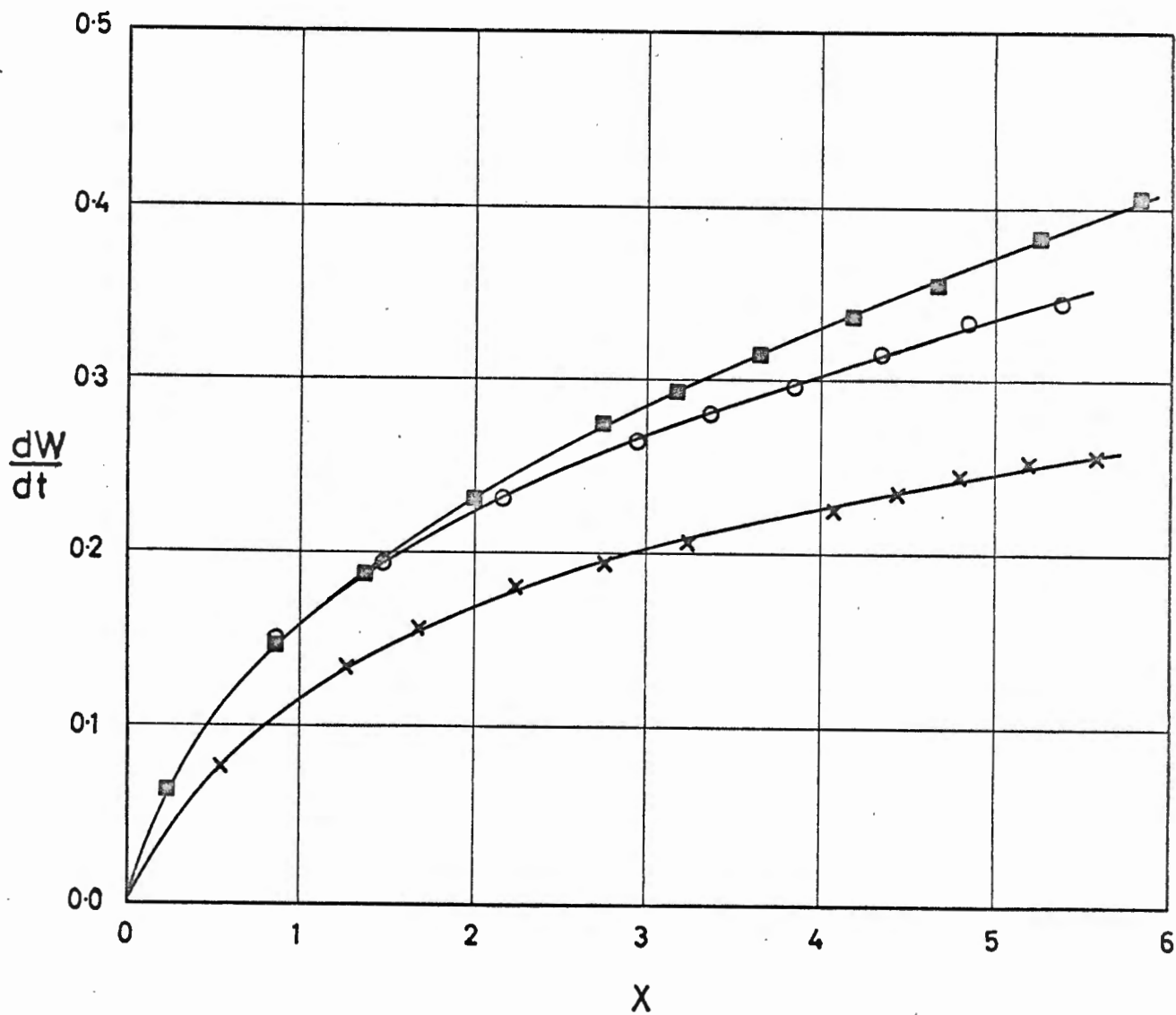


Fig. 21 The Effect of Air Velocity on the Drying Rates of 6.4 mm Thick Apple Ring Slices at 40 Percent Relative Humidity.

	<u>Air Velocity</u>	<u>Run No.</u>
■	232 m/min	3
○	183 m/min	21
×	122 m/min	23

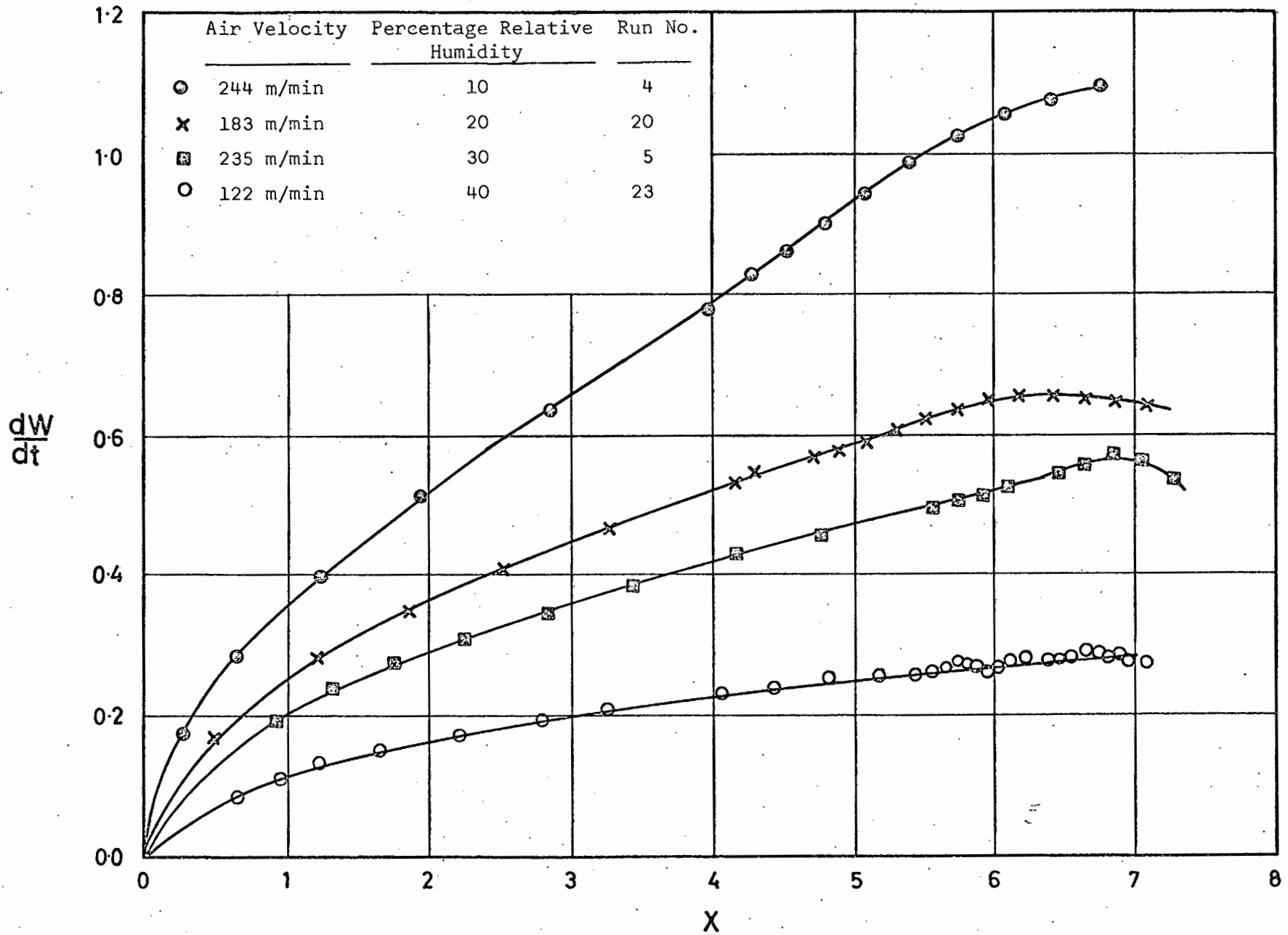


Fig. 22 Drying Rates determined at High Apple Ring Moisture Contents (6.4 mm Thick Slices), in an Attempt to show Constant-Rate Drying.

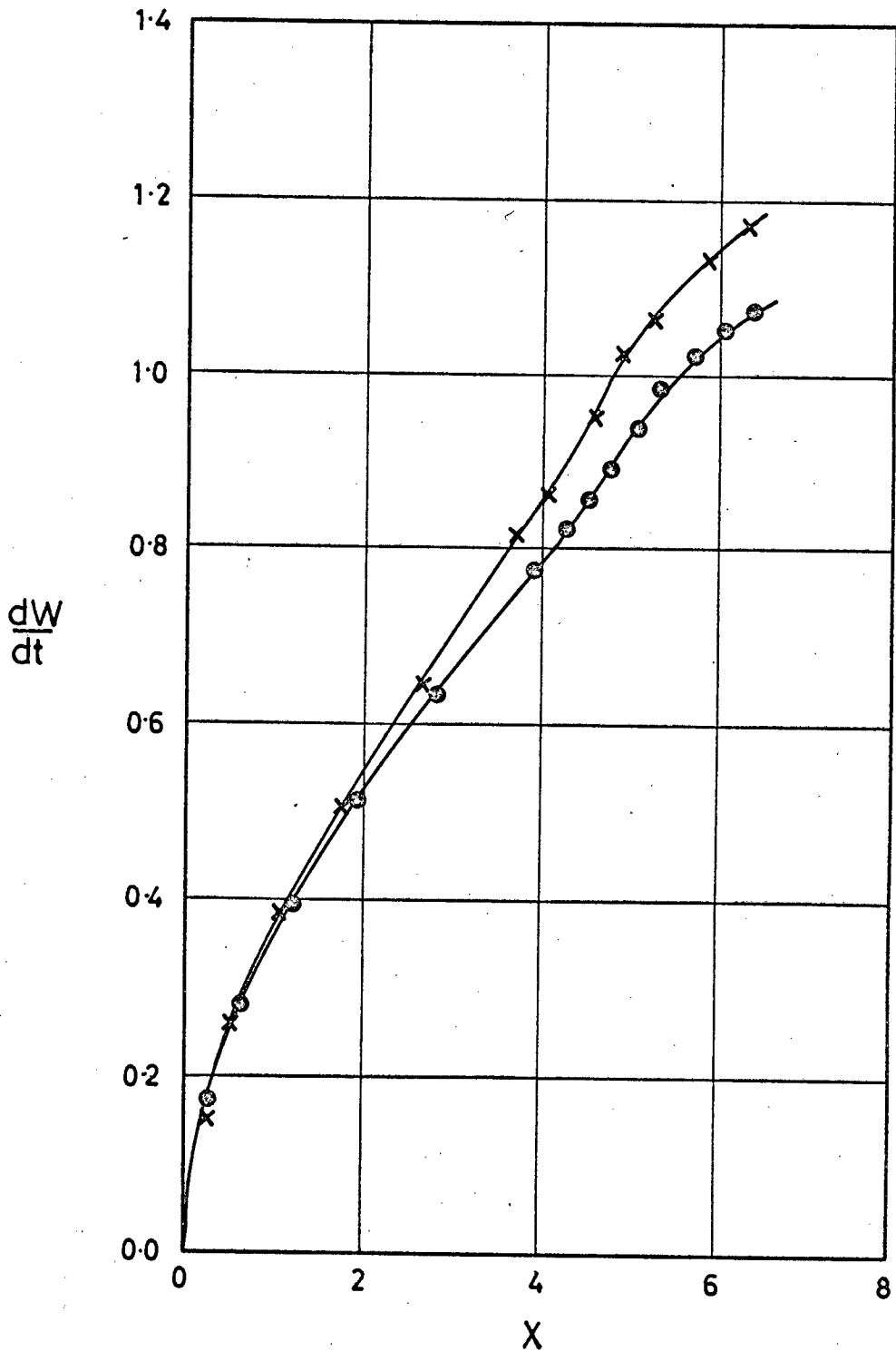


Fig. 23 Curves showing the Effect of Packed Length on the Drying Rates of 6.4 mm Thick Apple Ring Slices at 10 Percent Relative Humidity.

- × 115 mm packed length Run No. 24
- ⊙ 230 mm packed length Run No. 4

half of the packed length of fruit used in previous work.

Rate curves obtained on the plastic-coated, wire tray and dried under similar controlled conditions, differed significantly when the packed length of apple rings was halved. Fig. 23 shows the results found for 6.4 mm. thick apple slices, at 10 percent relative humidity. From Fig. 23 it may be concluded that the effect, of finite packed length of the fruit being dried, is more pronounced at higher drying rates. This is in accordance with expectation, since at the high drying rates a larger temperature differential (about 2.5°C) existed over the apple ring load. This differential tends to retard the overall drying rate somewhat, because the average humidity over the apple load will be noticeably higher than the inlet humidity for the tray. So for a longer packed length this effect is more marked.

From the above discussion it is clear that an assumption of point-drying conditions, when using any of the rate curves, is an approximation. But, nevertheless, as long as the rate results are correctly used as an average drying rate over 230 mm. they can be successfully applied to gain information on the industrial drying process.

5. 10 SIMULATION RUNS

In these runs 6.4 mm. thick apple slices were dried under conditions which simulated the parallel-flow industrial dehydrator drying process. The total drying cycle in an industrial dehydrator is between roughly 6 to 9 hours. By comparing the rate results for open and closed tray surfaces, since drying is far more rapid in the former case, a realistic total drying time of 3.5 hours was used when simulating the parallel-flow industrial dehydrator.

The apple rings were dried in each simulated position for one tenth of the total drying time (because the dehydrator being simulated had 10 trucks of trays). The output dry-bulb temperature, from a simulated tray position, may be considered as the input temperature to the next tray position. Thus temperatures were monitored continuously at the tray outlet, for each of the drying periods, and used as the input temperatures to the following simulated tray position.

A tray spacing of 76 mm. was used between each of the 3 trays (discussed in section 3.4). Typical industrial conditions were used as the input to the first tray position and are: an air velocity of 240 m/min, a dry-bulb temperature of 77.3°C and a wet-bulb temperature of 37.8°C - these temperatures correspond to 10 percent relative humidity. The mass velocity of dry air was kept constant for the 10 simulated tray positions, as was the wet-bulb temperature (due to an assumption of adiabatic drying conditions).

In the runs performed it was difficult to produce the exact input conditions of temperature and humidity (obtained from the output temperatures of the previous simulated tray position), because the control systems did not respond very well to the dynamically changing set-point of the dry-bulb temperature. However, the best of the results does show that after the total drying cycle, the air dry-bulb temperature had been depressed to about 59°C and the average total moisture content of the product apple rings was : $X_T = 0.114$ (this corresponds to a moisture content of 10.2 percent). Moisture content stipulations for commercially dried apple rings is that they should contain less than 18 percent moisture.

Thus, in this run, the apple rings had dried adequately in 3.5 hours.

This technique is a powerful means of obtaining reliable design and operating information.

5.11 APPLICATION OF THE RESULTS OBTAINED UNDER CONSTANT EXTERNAL DRYING CONDITIONS.

In an endeavour to simulate the industrial dehydration process by computational means, the drying rate results obtained under constant external conditions, were applied in the form of the normalized curve given by Eqn. (10). It was envisaged that if this method could be developed sufficiently enough to obtain reliable design information, it would overcome the necessity to do actual experimental simulation work (which takes a relatively long time to do and involves much preparation).

The principle of the computer simulation program is

essentially to consider drying over a differential length of the tray, during a short period of time. A heat and material balance give the output conditions of temperature and absolute humidity, H_a (g water/g dry-air), from this section - these are the input conditions to the subsequent tray section. This procedure was applied for each of the imaginary sections, into which the trays were divided, and for all of the 10 simulated tray positions.

Assumptions made in the program are:

1. Complete mixing of the air between the trays to give a uniform temperature and humidity.
2. Data obtained under constant drying conditions was applicable and that the non-point-drying condition, under which these results were obtained, could be compensated for in the computational procedure.

Details of the actual programming techniques used, are given in Appendix D.

In the computational simulation runs that were investigated, a total drying time of 3.5 hours was used. The input conditions of the air to the first tray were: an air velocity of 240 m/min. and an absolute humidity equivalent to a relative humidity of 10 percent at a dry-bulb temperature of 77.3°C . Drying 6.4 mm. apple slices on 0.915 m. long trays, was considered. These conditions are identical to those of the experimental simulation runs that were performed and which are discussed in section 5.10.

The most satisfactory results were obtained when the tray was subdivided into 4 imaginary drying sections and drying considered in each of these sections, and subsequently, for all of the 10 simulated tray positions. The resultant average, total moisture content of the product apple rings, according to computation, was $X_T = 0.123$ (which corresponds to a moisture content of 11.0 percent). This is in good agreement with the resultant moisture content found by experimental simulation (i.e. $X_T = 0.114$). However, the output temperatures from the simulated tray positions, obtained by the 2 different techniques, do not compare too well. Fig. 23 shows a plot, of the input and output

temperatures to and from each of the 10 trays, found by both computational and experimental means. The computed dry-bulb temperatures are consistently lower than those obtained experimentally. Also significant was the absence, in the experimental results, of the saw-tooth-like change in temperature with time (or position). These discrepancies are probably explained by the fact that initial control of the wet- and dry-bulb temperatures was not as good as it could have been.

Clearly, further work should be done, to develop both the computational and experimental simulation techniques, to an extent that the results obtained from either method are applicable to the design of the industrial dehydrator.

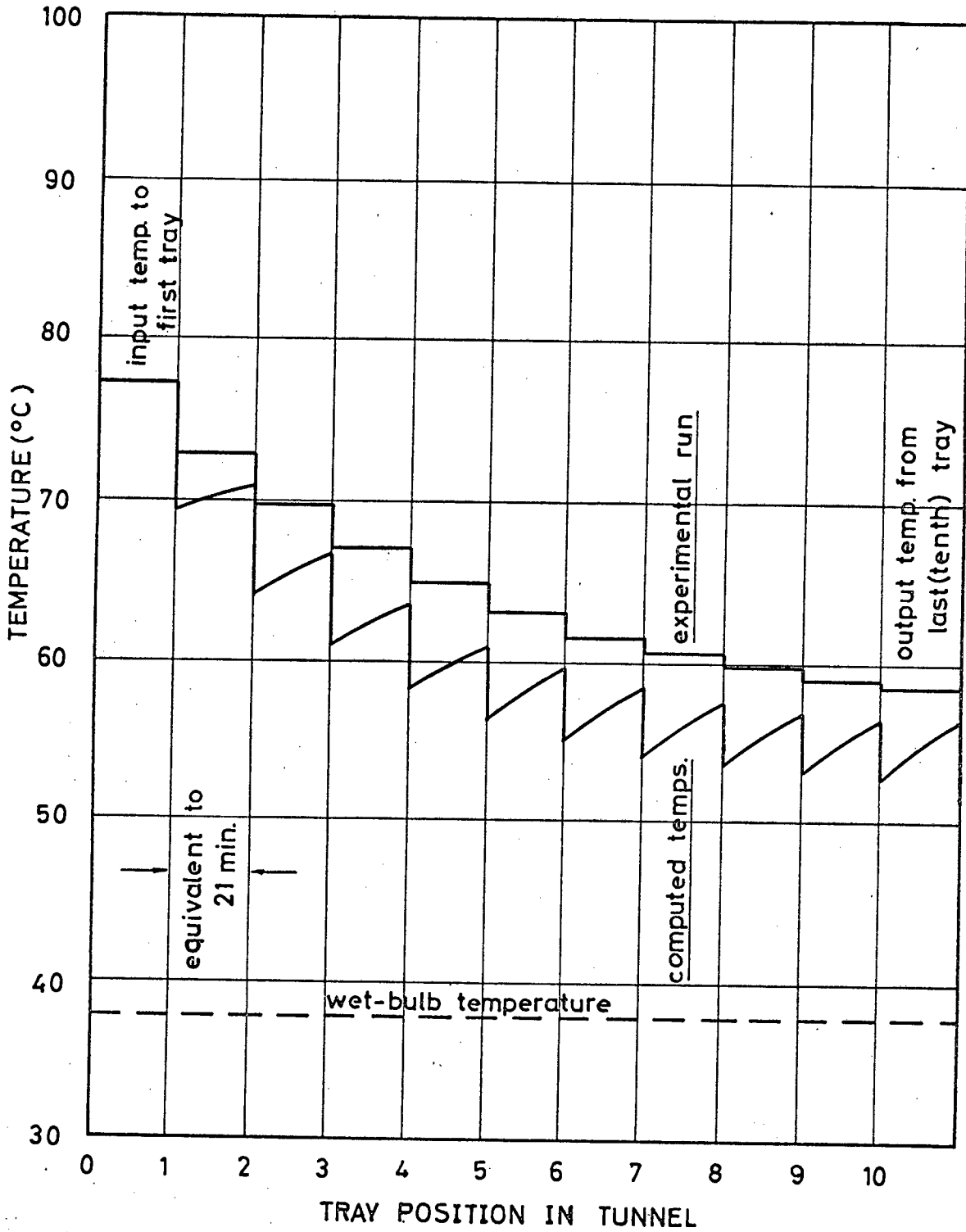


Fig. 24 Input and Output Temperatures to and from Trays in Different Positions in the Simulated Tunnel, found by Computational and Experimental Simulation of the Industrial Drying Process.

CHAPTER 6

CONCLUSIONS AND RECOMMENDATIONS

6.1 CONCLUSIONS

This investigation into apple ring dehydration yielded information of theoretical and practical value. Drying rate curves, for any specific apple ring thickness, were successfully normalized (to give a single curve) by an equation of the form:

$$\frac{dw}{dt} \left[0.01(Hr^* - Hr)ps \right]^B = AX_T^C \quad (10)$$

This type of equation can be used to calculate the drying rate of apple rings, for a particular slice thickness, for any feasible value of driving force or total moisture content. Furthermore, Eqn. (10) may be used to obtain design and operation information for the development of a more efficient and economic industrial dehydrator.

The equilibrium moisture content curve was found and the resultant fitted curve facilitates the calculation of the equilibrium moisture content at any value of air relative humidity (providing that cases are considered at a wet-bulb temperature of 37.8°C).

Trends, illustrating the effect of velocity, tray surface and apple slice thickness on drying rates, were established. Of particular interest was the fact that drying on an open tray surface, such as a plastic-coated wire tray, is far superior to drying on a solid tray surface, such as a wooden tray. The drying rates found for the former type of tray surface, at any value of air humidity, are much higher than those obtained for the latter case. A further advantage, of the plastic-coated wire tray, is that the product apple rings do not stick to the tray as they do with the industrially used wooden tray. Thus, if a cheap, light, but structurally sound plastic-coated wire tray could be developed for industrial drying purposes, it would be a great improvement on the existing wooden trays.

6.2 RECOMMENDATIONS

There are a number of recommendations that can be made with

regard to future experimental work and improvements that could be made on existing equipment. If sufficient reliable data, oriented towards practical application, is accumulated it will eventually lead to complete optimization of the design and operation of the industrial dehydrator.

Some recommendations are:

(i) A more comprehensive investigation should be made into the effect of apple slice thickness on drying rates. This will enable correlation of slice thickness with drying rate, total moisture content and driving force. The effect of the number of layers of apple rings, spread on the tray, also deserves attention.

(ii) Additional experimental work needs to be done on the effect of humidity on drying, especially at elevated dry-bulb temperatures. Coupled with this, attention should be paid to the effect of wet-bulb temperature on the drying characteristics of apple rings. Certainly, the influence of the wet-bulb temperature on the equilibrium moisture content curve should be established.

(iii) More knowledge, on the effect of air valocity on drying rates, is required.

(iv) There are a host of variables, concerned with the preparation of the apple rings, that warrant investigation; for example: sulphur dioxide penetration into the apple rings, the best concentration of sodium metabisulphite to use in the preparation solution, the optimum periods for dipping and draining the prepared apple rings, the sulphur dioxide loss from the rings during drying, etc.

(v) The drying characteristics of different varieties of apples should be determined.

(vi) More work is necessary on the experimental simulation of the industrial drying process. It is recommended that the on-off wet-bulb control system be replaced by a more effective controller, which will control steam input into the wind-tunnel.

NOMENCLATURE

A	constant
a	constant
B	constant
b	constant
C	constant
c	constant
D	bone-dry weight of apple sample taken for vacuum oven analysis, g bone-dry apple.
D ₁	bone-dry load of apple rings on tray, g bone-dry apple/m ² .
D.F.	driving force, mm. mercury pressure.
d	latent heat of vaporization of water, cal/g.
$\frac{dw}{dt}$	drying rate of apple rings, g/m ² sec.
E ₁	weight of dish used in vacuum oven analyses (of moisture content of apple rings), g.
E ₂	weight of dish plus samples, before vacuum drying, g.
E ₃	weight of dish plus sample, after vacuum drying, g.
e	constant
f	constant
g	constant
Ha	absolute humidity, g water/g bone-dry air.
Ha ₁	input absolute humidity to a simulated tray section, g water/g bone-dry air.
Ha ₂	output absolute humidity from a simulated tray section, g water/g bone-dry air.
Ha _i	any value of absolute humidity in an adiabatic process, g water/g bone-dry air.
Hr	percentage relative humidity of air
Hr*	percentage relative humidity of air equilibrated with apple rings of equilibrium moisture content, X _T *.
n	constant
p	partial pressure of water vapour in the air, mm. mercury.
p*	potential partial pressure of water that apple rings would exert if they were allowed to equilibrate with the air at a total moisture content (in the fruit) of X _T

ps	vapour pressure of water, mm. mercury.
R	resistance to mass transfer in apple rings.
T	air temperature, °C.
T ₁	input temperature to a simulated tray section, °C.
T ₂	output temperature from a simulated tray section, °C.
T _i	any value of air temperature in an adiabatic process, °C.
t	time, hr.
W	weight of apple sample taken for vacuum oven analysis, g.
W ₁	final load of product apple rings on tray, g/m ²
W ₂	load of apple rings on tray at any time during drying, g/m ² .
X	free moisture content, g water/g bone-dry solid.
X _T	total moisture content, g water/g bone-dry solid
X _{T1}	final moisture content of product apple rings on tray, g water/g bone-dry apple.
X _T *	equilibrium moisture content, g water/g bone-dry solid.
y	mole fraction of water vapour in the air, dimensionless.

LIST OF REFERENCES

- [1] Perry, R.I., Mrazk, E.M., Phaff, H.J., Marsh, G.L., and Fisher, G.D. "Fruit Dehydration", Bulletin 698, College of Agriculture, Univ. California, Berkeley (1946), p. 8.
- [2] Von Loesecke, H.W., "Drying and Dehydration of Foods", Reinhold, New York (1943), p.38.
- [3] Gentry, J.P., Claypool, L.L., and Miller, M.W., "Parallel-Flow Prune Dehydration", California Agriculture, 19, 8, (1965), p.12.
- [4] Kilpatrick, P.W., Lowe, E., and van Arsdel, W.B., "Advances in Food Research", 6, Academic Press, New York (1955), p.318.
- [5] Ibid, p.337.
- [6] McCabe, W.L., and Smith, J.C., "Unit Operations of Chemical Engineering", McGraw-Hill, New York (1956), p.887.
- [7] Ibid, p.898.
- [8] Van Arsdel, W.B., "Food Dehydration", 1, Avi, Westport, Connecticut (1963), p.24.
- [9] Ower, E., and Parkhurst, R.C., "The Measurement of Air Flow", 4th ed., Pergamon Press, Oxford (1966), p.107.
- [10] Ibid, p.198.
- [11] Ibid, p.200.
- [12] Von Loesecke, H.W., op.cit. Ref. [2], p.41.
- [13] Van Arsdel, W.B., op.cit. Ref. [8], p.174
- [14] Ibid, p.109.
- [15] Kilpatrick, P.W., op.cit. Ref. [4], p.327.
- [16] Ibid, p.327.

APPENDICES

- APPENDIX A EQUILIBRIUM MOISTURE CONTENT DATA
- APPENDIX B CALCULATION OF TOTAL MOISTURE CONTENT
- APPENDIX C DRYING RATE COMPUTATION AND TABULATION
- APPENDIX D EXPLANATION OF THE COMPUTER PROGRAM USED TO
SIMULATE THE DEHYDRATOR DRYING PROCESS.

APPENDIX A.

EQUILIBRIUM MOISTURE CONTENT DATA

Below is tabulated data on equilibrium moisture contents, X_T^* , obtained at different air percentage relative humidities, Hr^* , at a wet-bulb temperature of 37.8°C . These data points are plotted on the graph in Fig. 11.

Hr^*	X_T^*
100	6.809
100	6.530
100	7.210
100	6.628
94	0.817
80	0.328
70	0.229
60	0.176
50	0.133
50	0.126
40	0.084
40	0.102
30	0.060
30	0.061
30	0.079
20	0.042
20	0.044
20	0.056
10	0.028
10	0.034

APPENDIX B

CALCULATION OF TOTAL MOISTURE CONTENT

B.1 SAMPLE CALCULATION USED IN MOISTURE CONTENT ANALYSES

Whenever a load of apple rings was analysed for moisture content, 3 samples were taken. The results of the 3 moisture content analyses were averaged to give the value used in further calculations.

A sample calculation of moisture content is given below:

Each analysis involves 3 weight readings, typical values of which are:

Weight of empty drying dish, E_1 : 45.010 g

Weight of dish + sample, prior to vacuum drying, E_2 : 61.696 g

Weight of dish + sample, after vacuum drying, E_3 : 59.748 g

The total moisture content, X_T , is given by:

$$X_T = \frac{E_2 - E_3}{E_3 - E_1} \quad (B1)$$

Substituting the above weights into Eqn. (B1), yields:

$$X_T = \frac{61.696 - 59.748}{59.748 - 45.010} = 0.132 \text{ [g water/g bone-dry apple]}$$

B.2 CALCULATION OF TOTAL MOISTURE CONTENT OF THE APPLE RINGS DURING DRYING:

Consider the situation where, after 3 hours of drying, the load of apple rings on the drying tray was 1835.7 g/m². In addition, when drying was terminated the load of apple rings, W_1 , on the tray was 670.5 g/m². Compute the value of total moisture content after 3 hours of drying, if the moisture content of the product apple rings, X_{T1} , was 0.132 [g water/g bone-dry apple]

From Eqn. (15), the bone-dry weight, D , of the apple load is:

$$D_1 = \frac{W_1}{1 + X_{T1}} \quad (15)$$

$$D_1 = \frac{670.5}{1 + 0.132} = 592.3 \text{ [g bone-dry apple/m}^2\text{]}$$

The value of total moisture content at any time during drying may be calculated from Eqn. (14):

$$X_T = \frac{W_2 - D_1}{D_1} \quad (14)$$

Thus after 3 hours of drying (in case mentioned above), the total moisture content of the apple ring load was:

$$X_T = \frac{1835.7 - 592.3}{592.3} = 2.099 \text{ [g water/g bone-dry apple]}$$

APPENDIX C

DRYING RATE COMPUTATION AND TABULATION

C.1 SAMPLE CALCULATION OF DRYING RATE

Below is given a sample calculation of a drying rate (of apple rings), given 5 typical data points of weight of the apple load (in g/m²) versus time (in hours):

TIME	WEIGHT
0.50	4709.1
0.75	4144.3
1.00	3633.7
1.25	3204.9
1.50	2818.3

These results are taken from Table C.13 in Appendix C.

A second order equation was fitted to 5 data points at a time. The form of the equation was:

$$W = a + bt + ct^2 \quad (C)$$

The coefficients of Eqn. (C), using the data above, were found to be:

$$a = 6028.7$$

$$b = -2890.0$$

$$c = 500.8$$

The value of the weight of the load, at 1 hour, as computed from the fitted curve, is:

$$W = 3639.5 \text{ [g/m}^2\text{]}$$

The drying rate at 1 hour is given by the slope of the fitted curve at 1 hour and is:

$$\frac{dw}{dt} = -1888.4 \text{ g/m}^2\text{hr.}$$

or

$$\frac{dw}{dt} = -0.5246 \text{ g/m}^2\text{sec.}$$

The total moisture content, corresponding to the load on the tray after 1 hour of drying, may be calculated by the method shown in Appendix B. Thus weight data versus time may be converted to drying rates versus total moisture contents - these quantities form the basic ingredients for further calculation and discussion.

C.2 TABULATION OF DRYING RATE RESULTS

Experimental measurements and calculations, referring to drying rate determinations under different conditions, are tabulated in Tables C.1 to C.24. In these tables, drying times are given in hours, apple load weight in $[g/m^2]$, drying rates in $[g/m^2sec]$, moisture contents in $[g \text{ water}/g \text{ bone-dry apples}]$ and humidities are expressed in terms of percentage relative humidity.

All results were obtained using the same wet-bulb temperature of $37.8^{\circ}C$. Most results were obtained using a packed length of apple rings of approximately 230 mm, except for results given in Table C.24 - here, a packed length of 115 mm was used.

TABLE C 1

Run No. 1
 Air relative humidity 10 percent
 Air velocity 244 m/min
 Apple slice thickness 6.4 mm
 Type of tray plastic-coated, wire tray

TIME	WEIGHT	RATE	X_T	X	(Hr* - Hr)
0.00	4354.4		6.337	6.315	90.00
0.75	3498.2	0.9123	4.894	4.872	89.90
0.50	2712.7	0.7657	3.571	3.549	89.49
0.75	2118.3	0.6190	2.569	2.547	88.88
1.00	1630.6	0.4858	1.747	1.726	87.80
1.25	1253.8	0.3739	1.113	1.091	85.72
1.50	958.7	0.2645	0.615	0.594	80.61
1.75	771.7	0.1748	0.300	0.279	67.75
2.00	681.6	0.0932	0.149	0.127	45.97
2.50	634.5	0.0280	0.069	0.047	20.21
3.00	624.8	0.0092	0.053	0.031	13.22
4.00	616.5	0.0018	0.039	0.017	6.83
4.50	615.1		0.036	0.015	5.44
5.50	613.7		0.034	0.012	4.52

TABLE C 2

Run No. 2
Air relative humidity 20 percent
Air velocity 238 m/min
Apple slice thickness 6.4 mm
Type of tray plastic-coated, wire tray

TIME	WEIGHT	RATE	X_T	X	(Hr* - Hr)
0.00	4276.8		6.895	6.851	80.00
0.25	3690.8	0.6956	5.813	5.769	80.00
0.50	3122.7	0.6223	4.765	4.720	79.87
0.75	2567.2	0.5491	3.739	3.695	79.56
1.00	2112.8	0.4747	2.900	2.856	79.13
1.25	1724.9	0.3985	2.184	2.140	78.48
1.50	1407.6	0.3356	1.599	1.554	77.47
1.75	1126.4	0.2708	1.079	1.035	75.53
2.00	901.9	0.2093	0.665	0.620	71.49
2.50	662.2	0.1078	0.223	0.178	49.45
3.00	597.1	0.0483	0.102	0.058	22.77
4.50	575.0	0.0038	0.061	0.017	6.75
5.25	572.2		0.056	0.012	4.56
6.00	572.2		0.056	0.012	4.56

TABLE C 3

Run No. 3
 Air relative humidity 40 percent
 Air velocity 232 m/min
 Apple slice thickness 6.4 mm
 Type of tray plastic-coated, wire tray

TIME	WEIGHT	RATE	X _T	X	(Hr* - Hr)
0.00	4809.9		7.090	6.992	60.00
0.25	4493.4	0.4303	6.557	6.460	60.00
0.50	4111.9	0.4066	5.915	5.818	60.00
0.75	3760.7	0.3830	5.325	5.228	59.99
1.00	3428.2	0.3583	4.766	4.669	59.87
1.25	3111.7	0.3382	4.233	4.136	59.73
1.50	2824.1	0.3152	3.750	3.652	59.56
1.75	2540.8	0.2949	3.273	3.176	59.35
2.00	2295.1	0.2717	2.860	2.763	59.10
2.50	1845.6	0.2300	2.104	2.007	58.38
3.00	1461.2	0.1898	1.458	1.360	57.00
3.50	1156.2	0.1480	0.945	0.847	54.64
4.50	779.0	0.0656	0.310	0.213	38.54
5.00	711.1	0.0407	0.196	0.099	25.43
5.50	683.6		0.150	0.053	16.25
6.25	666.3		0.121	0.023	8.67

TABLE C 4

Run No. 4
 Air relative humidity 10 percent
 Air velocity 244 m/min
 Apple slice thickness 6.4 mm
 Type of tray plastic-coated, wire tray

TIME	WEIGHT	RATE	X_T	X	(Hr ² - Hr)
0.00	4509.1		7.043	7.021	90.00
0.05	4345.0	1.0967	6.776	6.754	90.00
0.10	4148.1	1.0763	6.422	6.400	90.00
0.15	3958.3	1.0559	6.083	6.062	90.00
0.20	3768.6	1.0242	5.740	5.718	90.00
0.25	3584.5	0.9870	5.414	5.392	90.00
0.30	3413.2	0.9402	5.106	5.084	89.95
0.35	3247.7	0.8958	4.811	4.789	89.88
0.40	3090.8	0.8593	4.528	4.506	89.81
0.45	2939.5	0.8225	4.258	4.237	89.74
0.50	2793.9	0.7785	3.996	3.975	89.65
0.75	2164.7	0.6351	2.866	2.844	89.11
1.00	1658.1	0.5134	1.958	1.936	88.17
1.25	1251.4	0.3962	1.227	1.205	86.27
1.50	940.4	0.2813	0.665	0.643	81.49
1.75	740.6	0.1727	0.303	0.281	67.98
2.00	647.8		0.130	0.108	41.23
2.25	670.7		0.084	0.063	26.18

TABLE C 5

Run No. 5
 Air relative humidity 30 percent
 Air velocity 235 m/min
 Apple slice thickness 6.4 mm
 Type of tray plastic-coated, wire tray

TIME	WEIGHT	RATE	X_T	X	(Hr* - Hr)
0.00	4461.6		7.532	7.463	70.00
0.05	4429.8	0.5070	7.485	7.416	70.00
0.10	4346.0	0.5333	7.325	7.256	70.00
0.15	4239.1	0.5597	7.121	7.051	70.00
0.20	4133.5	0.5725	6.919	6.849	70.00
0.25	4032.4	0.5572	6.725	6.656	70.00
0.30	3934.1	0.5420	6.535	6.465	70.00
0.40	3743.3	0.5259	6.170	6.100	70.00
0.45	3647.9	0.5107	5.985	5.915	70.00
0.50	3555.4	0.5020	5.808	5.738	70.00
0.55	3471.6	0.4905	5.647	5.578	70.00
0.80	3040.9	0.4569	4.821	4.751	69.88
1.00	2721.5	0.4260	4.210	4.141	69.72
1.25	2354.4	0.3850	3.508	3.439	69.46
1.50	2030.6	0.3441	2.886	2.817	69.12
1.75	1737.2	0.3083	2.322	2.253	68.64
2.00	1481.4	0.2725	1.836	1.766	67.96
2.25	1241.5	0.2359	1.374	1.305	66.83
2.75	890.3		0.703	0.633	62.08
3.00	770.3		0.473	0.404	56.95

TABLE C 6

Run No. 6
 Air relative humidity 20 percent
 Air velocity 238 m/min
 Apple slice thickness 7.9 mm
 Type of tray plastic-coated, wire tray

TIME	WEIGHT	RATE	X _T	X	(Hr ^{0.8} - Hr)
0.00	5158.2		6.941	6.897	80.00
0.25	4490.3	0.7748	5.913	5.868	80.00
0.50	3832.6	0.6834	4.900	4.856	79.90
0.75	3239.0	0.5919	3.987	3.942	79.65
1.00	2789.9	0.5031	3.295	3.250	79.36
1.25	2348.0	0.4278	2.615	2.570	78.92
1.50	2014.0	0.3712	2.101	2.056	78.37
1.75	1701.9	0.3147	1.620	1.575	77.52
2.00	1442.3	0.2703	1.221	1.176	76.24
2.25	1217.7	0.2223	0.875	0.830	74.06
2.50	1039.8	0.1750	0.601	0.556	70.32
2.75	902.7	0.1287	0.390	0.345	63.52
3.00	812.3	0.0862	0.251	0.206	52.95
3.50	736.5	0.0360	0.134	0.089	32.26
4.00	711.7		0.096	0.051	20.59
4.50	701.5		0.080	0.035	14.63

TABLE C 7

Run No. 7
 Air relative humidity 20 percent
 Air velocity 238 m/min
 Apple slice thickness 7.9 mm
 Type of tray plastic-coated, wire tray

TIME	WEIGHT	RATE	X_T	X	(Hr* - Hr)
0.00	5147.5		6.781	6.738	80.00
0.25	4459.5	0.7162	5.741	5.696	80.00
0.50	3860.7	0.6399	4.836	4.791	79.89
0.75	3294.9	0.5635	3.980	3.936	79.65
1.25	2444.2	0.4243	2.695	2.650	78.98
1.50	2091.6	0.3693	2.161	2.117	78.45
1.75	1782.1	0.3194	1.694	1.649	77.69
2.00	1517.2	0.2740	1.293	1.246	76.54
2.25	1294.1	0.2300	0.956	0.911	74.73
2.50	1102.6	0.1833	0.667	0.622	71.52
2.75	954.4	0.1396	0.443	0.398	65.85
3.00	862.2	0.0958	0.303	0.259	58.00
3.50	761.5	0.0430	0.151	0.106	36.56
4.00	729.8	0.0191	0.103	0.058	23.04
4.50	719.7	0.0071	0.088	0.043	17.65
5.00	711.1		0.075	0.030	12.63
5.50	706.8		0.068	0.024	9.75

TABLE C 8

Run No. 8
 Air relative humidity 40 percent
 Air velocity 232 m/min
 Apple slice thickness 7.9 mm
 Type of tray plastic-coated, wire tray

TIME	WEIGHT	RATE	X_T	X	(Hr* - Hr)
0.00	5239.7		6.942	6.845	60.00
0.25	4928.0	0.4003	6.469	6.372	60.00
0.50	4571.9	0.3829	5.930	5.833	60.00
0.75	4242.2	0.3651	5.430	5.333	60.00
1.00	3915.2	0.3454	4.935	4.837	59.91
1.25	3613.2	0.3271	4.477	4.380	59.80
1.50	3331.9	0.3008	4.050	3.953	59.67
1.75	3061.8	0.2829	3.641	3.544	59.52
2.00	2837.4	0.2652	3.301	3.204	59.36
2.50	2369.1	0.2352	2.591	2.494	58.90
3.00	1983.9	0.2080	2.007	1.910	58.24
3.50	1626.5	0.1757	1.465	1.368	57.11
4.00	1336.9	0.1441	1.027	0.929	55.21
4.50	111.1	0.1092	0.684	0.587	51.80
5.00	944.9	0.0758	0.432	0.335	45.43
5.50	839.6	0.0453	0.273	0.175	35.27
5.75	806.3	0.0331	0.222	0.125	29.41
6.00	782.8	0.0225	0.187	0.089	23.81
6.25	767.5		0.163	0.066	19.23
6.50	757.8		0.149	0.052	16.09

TABLE C 9

Run No 9
 Air relative humidity 40 percent
 Air velocity 232 m/min
 Apple slice thickness 7.9 mm
 Type of tray plastic-coated, wire tray

TIME	WEIGHT	RATE	X_T	X	(Hr* - Hr)
0.00	5218.1		6.559	6.462	60.00
0.25	4925.9	0.3873	6.136	6.039	60.00
0.50	4588.1	0.3735	5.647	5.550	60.00
0.75	4267.4	0.3597	5.182	5.085	59.96
1.00	3922.5	0.3408	4.682	4.585	59.85
1.25	3640.3	0.3188	4.274	4.176	59.74
1.50	3368.0	0.2949	3.879	3.782	59.61
1.75	3110.0	0.2815	3.506	3.408	59.46
2.00	2860.6	0.2676	3.144	3.047	59.28
2.50	2404.5	0.2341	2.483	2.286	58.80
3.00	2026.8	0.2010	1.936	1.839	58.13
3.50	1680.4	0.1691	1.434	1.337	57.02
4.00	1413.9	0.1391	1.048	0.951	55.35
4.50	1188.7	0.1080	0.722	0.625	52.35
5.00	1020.5	0.0794	0.478	0.381	47.13
5.50	905.1	0.0526	0.311	0.214	38.62
6.00	840.9	0.0312	0.218	0.121	28.87
6.50	805.3	0.0166	0.167	0.069	19.99
7.00	789.6		0.144	0.047	14.88
7.50	781.1		0.132	0.034	11.78

TABLE C 10

Run No. 10
 Air relative humidity 40 percent
 Air velocity 232 m/min
 Apple slice thickness 9.5 mm
 Type of tray plasticcoated, wire tray

TIME	WEIGHT	RATE	X_T	X	(Hr* - Hr)
0.00	6152.7		6.780	6.683	60.00
0.25	5906.1	0.4058	6.469	6.371	60.00
0.50	5551.4	0.3880	6.020	5.923	60.00
0.75	5207.8	0.3702	5.586	5.488	60.00
1.00	4882.2	0.3545	5.174	5.077	59.96
1.25	4574.7	0.3368	4.785	4.688	59.88
1.50	4272.6	0.3210	4.403	4.306	59.78
1.75	3997.0	0.3060	4.054	3.957	59.67
2.00	3726.8	0.2895	3.713	3.616	59.55
2.50	3229.4	0.2581	3.084	2.987	59.25
3.00	2801.3	0.2301	2.542	2.445	58.85
3.50	2420.3	0.2011	2.061	1.963	58.32
4.00	2060.1	0.1746	1.605	1.508	57.48
4.50	1790.0	0.1493	1.264	1.166	56.42
5.00	1544.7	0.1241	0.953	0.856	54.71
5.50	1334.2	0.1021	0.687	0.590	51.85
6.00	1170.7	0.0774	0.480	0.383	47.19
6.50	1058.5	0.0541	0.339	0.241	40.57
7.00	986.4	0.0354	0.247	0.150	32.59
7.50	939.3	0.0219	0.188	0.091	24.05
8.00	911.6	0.0127	0.153	0.056	16.97
8.50	899.1		0.137	0.040	13.10
9.00	892.2		0.128	0.031	10.68

TABLE C 11

Run No. 11
 Air relative humidity 40 percent
 Air velocity 232 m/min
 Apple slice thickness 9.5 mm
 Type of tray plastic-coated, wire tray

TIME	WEIGHT	RATE	X_T	X	(Hr* - Hr)
0.00	6054.3		6.666	6.569	60.00
0.25	5773.2	0.3962	6.310	6.212	60.00
0.50	5417.7	0.3784	5.860	5.762	60.00
0.75	5089.2	0.3606	5.444	5.346	60.00
1.00	4778.3	0.3427	5.050	4.953	59.93
1.25	4470.1	0.3279	4.660	4.563	59.85
1.50	4184.9	0.3133	4.299	4.201	59.75
1.75	3910.5	0.2958	3.951	3.854	59.64
2.00	3648.3	0.2805	3.620	3.522	59.51
2.50	3177.9	0.2515	3.024	2.926	59.21
3.00	2744.0	0.2251	2.474	2.379	58.79
3.50	2368.2	0.1987	1.999	1.901	58.23
4.00	2027.6	0.1726	1.567	1.470	57.39
4.50	1747.8	0.1475	1.213	1.116	56.21
5.00	1500.4	0.1230	0.900	0.803	54.28
5.50	1304.4	0.0981	0.652	0.554	51.27
6.00	1142.2	0.0737	0.446	0.349	45.98
6.50	1043.5	0.0513	0.321	0.224	39.37
7.00	967.8		0.225	0.128	29.79
7.50	930.0		0.178	0.080	22.25

TABLE C 12

Run No. 12
 Air relative humidity 20 percent
 Air velocity 239 m/min
 Apple slice thickness 9.5 mm
 Type of tray plastic-coated, wire tray

TIME	WEIGHT	RATE	X _T	X	(Hr* - Hr)
0.00	5880.1		6.330	6.285	80.00
0.25	5216.2	0.7299	5.502	5.458	80.00
0.50	4586.0	0.6545	4.717	4.672	79.86
0.75	4039.8	0.5790	4.036	3.991	79.67
1.00	3549.7	0.5054	3.425	3.380	79.43
1.25	3129.0	0.4428	2.900	2.856	79.13
1.50	2767.1	0.3862	2.449	2.405	78.77
1.75	2438.6	0.3432	2.040	1.995	78.29
2.00	2156.8	0.3055	1.689	1.644	77.67
2.50	1665.3	0.2345	1.074	1.030	75.50
3.00	1308.2	0.1665	0.631	0.587	70.91
3.50	1073.7	0.1040	0.338	0.294	60.56
4.00	955.6	0.0638	0.189	0.144	44.19
4.50	910.8	0.0301	0.129	0.084	30.87
6.00	873.1		0.082	0.037	15.41
6.50	862.7		0.075	0.031	12.63

TABLE C 13

Run No. 13
 Air relative humidity 20 percent
 Air velocity 238 m/min
 Apple slice thickness 9.5 mm
 Type of tray plastic-coated, wire tray

TIME	WEIGHT	RATE	X_T	X	(Hr* - Hr)
0.00	5991.6		6.737	6.693	80.00
0.25	5350.3	0.7483	5.909	5.865	80.00
0.50	4709.1	0.6723	5.081	5.036	79.94
0.75	4144.3	0.5962	4.352	4.307	79.76
1.00	3633.7	0.5246	3.693	3.648	78.54
1.25	3204.9	0.4592	3.139	3.094	79.28
1.50	2818.3	0.4021	2.640	2.595	78.94
1.75	2485.8	0.3566	2.210	2.165	78.51
2.00	2183.7	0.3136	1.820	1.775	77.93
2.50	1692.8	0.2434	1.186	1.141	76.08
3.00	1308.9	0.1742	0.690	0.646	71.89
3.75	979.0	0.0821	0.264	0.220	54.43
4.00	932.8	0.0615	0.205	0.160	46.83
4.50	877.1		0.126	0.082	30.12
5.00	855.0		0.104	0.059	23.34

TABLE C 14

Run No. 14
 Air relative humidity 20 percent
 Air velocity 238 m/min
 Apple slice thickness 3.2 mm
 Type of tray plastic-coated, wire tray

TIME	WEIGHT	RATE	X_T	X	(Hr* - Hr)
0.00	2550.7		6.912	6.868	80.00
0.25	1915.1	0.7108	4.940	4.896	79.91
0.50	1354.2	0.5660	3.201	3.156	79.31
0.75	902.8	0.4213	1.800	1.756	77.90
1.00	575.6	0.2754	0.785	0.741	73.15
1.25	408.7	0.1457	0.268	0.223	54.77
1.50	361.9	0.0565	0.123	0.078	29.14
1.75	353.9	0.0154	0.098	0.053	21.22
2.00	348.6	0.0047	0.081	0.037	15.09
2.25	345.9		0.073	0.028	11.78
2.50	344.6		0.069	0.024	10.16

TABLE C 15

Run No. 15
 Air relative humidity 40 percent
 Air velocity 232 m/min
 Apple slice thickness 3.2 mm
 Type of tray plastic-coated, wire tray

TIME	WEIGHT	RATE	X_T	X	(Hr* - Hr)
0.00	2599.4		6.701	6.604	60.00
0.25	2272.2	0.4116	5.732	5.635	60.00
0.50	1915.6	0.3762	4.675	4.578	59.85
0.75	1599.1	0.3408	3.738	3.641	59.56
1.00	1300.4	0.3044	2.853	2.755	59.10
1.25	1046.2	0.2658	2.100	2.003	58.37
1.50	821.8	0.2206	1.435	1.338	57.02
1.75	647.1	0.1717	0.902	0.805	54.30
2.00	509.6	0.1219	0.510	0.413	48.10
2.25	429.8	0.0746	0.274	0.176	35.35
2.75	379.8		0.125	0.028	9.83
3.50	374.4		0.109	0.012	4.98

TABLE C 16

Run No. 16
Air relative humidity 40 percent
Air velocity 232 m/min
Apple slice thickness 6.4 mm
Type of tray closed, solid tray

TIME	WEIGHT	RATE	X_T	X
0.00	4522.9		6.601	6.504
0.25	4328.8	0.2872	6.275	6.177
0.50	4071.5	0.2772	5.842	5.745
0.75	3833.3	0.2671	5.442	5.345
1.00	3590.6	0.2546	5.034	4.937
1.25	3367.2	0.2432	4.659	4.561
1.75	2958.4	0.2174	3.972	3.874
2.50	2448.8	0.1863	3.065	2.968
3.00	2092.3	0.1647	2.516	2.420
3.50	1818.9	0.1440	2.057	1.959
4.25	1479.2	0.1151	1.486	1.389
4.50	1376.3	0.1065	1.313	1.216
5.00	1199.8	0.0906	1.016	0.919
5.50	1052.8	0.0745	0.769	0.672
6.00	937.2		0.567	0.469
7.00	774.9		0.302	0.205

TABLE C 17

Run No. 17
Air relative humidity 40 percent
Air velocity 232 m/min
Apple slice thickness 6.4 mm
Type of tray closed, solid tray

TIME	WEIGHT	RATE	X_T	X
0.00	4429.4		6.580	6.483
0.25	4265.0	0.2908	6.299	6.201
0.50	4017.0	0.2793	5.874	5.777
0.75	3766.2	0.2677	5.445	5.348
1.00	3525.2	0.2578	5.032	4.935
1.50	3050.4	0.2300	4.289	4.191
2.00	2697.5	0.2042	3.616	3.519
2.50	2360.3	0.1807	3.039	2.942
3.75	1918.6	0.1486	2.283	2.186
3.75	1665.0	0.1300	1.849	1.752
4.00	1559.1	0.1208	1.668	1.571
4.50	1354.3	0.1032	1.318	1.220
5.00	1184.3	0.0875	1.027	0.930
5.50	1042.2	0.0720	0.784	0.686
6.00	928.0	0.0577	0.588	0.491
6.50	834.6	0.0443	0.428	0.331
7.00	769.1		0.316	0.219
7.50	723.1		0.238	0.140

TABLE C 18

Run No. 18
Air relative humidity 20 percent
Air velocity 238 m/min
Apple slice thickness 6.4 mm
Type of tray closed, solid tray

TIME	WEIGHT	RATE	X_T	X
0.00	4393.2		6.863	6.818
0.25	3965.4	0.4851	6.097	6.053
0.50	3560.0	0.4380	5.372	5.327
0.75	3175.4	0.3909	4.683	4.639
1.00	2848.0	0.3505	4.097	4.053
1.25	2562.4	0.3126	3.586	3.541
1.50	2289.3	0.2804	3.097	3.053
1.75	2048.2	0.2533	2.666	2.621
2.00	1843.4	0.2239	2.299	2.255
2.50	1482.5	0.1804	1.653	1.609
3.00	1193.5	0.1432	1.140	1.095
3.75	884.8	0.0899	0.584	0.539
4.00	809.5	0.0750	0.449	0.404
4.50	710.6		0.272	0.227
5.00	652.1		0.167	0.122

TABLE C 19

Run No. 19
Air relative humidity 20 percent
Air velocity 238 m/min
Apple slice thickness 6.4 mm
Type of tray closed, solid tray

TIME	WEIGHT	RATE	X_T	X
0.00	4287.3		6.939	6.894
0.25	3871.2	0.5154	6.168	6.123
0.50	3429.3	0.4625	5.350	5.305
0.75	3033.1	0.4095	4.616	4.572
1.00	2699.5	0.3603	3.999	3.954
1.25	2393.1	0.3163	3.431	3.387
1.50	2128.0	0.2802	2.940	2.896
1.75	1895.7	0.2474	2.510	2.466
2.00	1687.8	0.2190	2.125	2.080
2.50	1341.2		1.484	2.439
3.00	1067.6		0.977	0.932

TABLE C 20

Run No. 20
Air relative humidity 20 percent
Air velocity 183 m/min
Apple slice thickness 6.4 mm
Type of tray plastic-coated, wire tray

TIME	WEIGHT	RATE	X_T	X
0.00	4326.6		7.341	7.297
0.05	4216.9	0.6401	7.130	7.085
0.10	4102.6	0.6472	6.910	6.865
0.15	3984.0	0.6543	6.681	6.636
0.20	3865.3	0.6576	6.452	6.407
0.25	3746.7	0.6567	6.223	6.179
0.30	3629.5	0.6518	5.997	5.953
0.35	3510.8	0.6382	5.769	5.724
0.40	3396.6	0.6213	5.549	5.504
0.45	3288.3	0.6040	5.340	5.295
0.50	3181.5	0.5850	5.134	5.089
0.55	3074.8	0.5780	4.928	4.883
0.60	2976.9	0.5676	4.739	4.695
0.70	2769.2	0.5422	4.339	4.294
0.75	2677.2	0.5292	4.162	4.117
1.00	2233.8	0.4612	3.307	3.262
1.25	1845.2	0.4050	2.557	2.513
1.50	1511.4	0.3479	1.914	1.869
1.80	1164.3	0.2800	1.245	1.200
2.25	795.0	0.1690	0.533	0.488
2.50	668.9		0.290	0.245
2.75	608.1		0.172	0.128

TABLE C 21

Run No. 21
Air relative humidity 40 percent
Air velocity 183 m/min
Apple slice thickness 6.4 mm
Type of tray plastic-coated, wire tray

TIME	WEIGHT	RATE	X_T	X
0.00	4612.0		7.127	7.030
0.05	4595.2	0.3931	7.097	7.000
0.10	4524.2	0.3909	6.972	6.875
0.15	4454.5	0.3886	6.849	6.752
0.20	4384.8	0.3870	6.727	6.629
0.25	4315.2	0.3855	6.604	6.507
0.30	4245.5	0.3785	6.481	6.384
0.35	4177.2	0.3661	6.361	6.264
0.40	4113.1	0.3576	6.248	6.151
0.45	4051.8	0.3522	6.140	6.043
0.50	3986.3	0.3545	6.024	5.927
0.55	3923.6	0.3560	5.914	5.817
0.60	3858.2	0.3499	5.798	5.701
0.65	3795.5	0.3452	5.688	5.591
0.70	3735.5	0.3401	5.582	5.485
0.75	3674.2	0.3444	5.474	5.377
1.00	3366.3	0.3323	4.932	4.835
1.25	3073.7	0.3147	4.416	4.319
1.50	2802.0	0.2974	3.937	3.840
1.75	2540.1	0.2801	3.476	3.379
2.00	2294.8	0.2640	3.044	2.947
2.50	1851.7	0.2310	2.263	2.166
3.00	1468.6	0.1947	1.588	1.491
3.55	1098.0	0.1499	0.935	0.838
4.25	809.5		0.427	0.329
4.75	702.2		0.237	0.140

TABLE C 22

Run No. 22
 Air relative humidity 20 percent
 Air velocity 122 m/min
 Apple slice thickness 6.4 mm
 Type of tray plastic-coated, wire tray

TIME	WEIGHT	RATE	X _T	X
0.00	4468.4		7.044	6.999
0.05	4432.2	0.5212	6.978	6.934
0.10	4337.5	0.5156	6.808	6.763
0.15	4244.1	0.5101	6.640	6.595
0.20	4157.7	0.5078	6.484	6.440
0.25	4063.0	0.5078	6.314	6.269
0.30	3971.0	0.5070	6.148	6.104
0.35	3880.5	0.5016	5.985	5.941
0.40	3792.7	0.4962	5.827	5.783
0.45	3700.7	0.4892	5.662	5.617
0.50	3614.3	0.4807	5.506	5.461
0.55	3529.3	0.4714	5.353	5.308
0.60	3445.7	0.4590	5.203	5.158
0.65	3360.7	0.4435	5.050	5.005
0.70	3285.5	0.4427	4.914	4.870
0.75	3210.3	0.4420	4.779	4.734
0.80	3122.5	0.4466	4.621	4.576
0.85	3044.4	0.4412	4.480	4.436
0.90	2955.4	0.4257	4.340	4.295
0.95	2891.2	0.4204	4.204	4.160
1.00	2815.9	0.4173	4.069	4.024
1.25	2450.9	0.3900	3.412	3.367
1.50	2112.3	0.3571	2.802	2.758
1.75	1805.7	0.3225	2.551	2.206
2.00	1531.3	0.2861	1.757	1.712
2.75	1290.2	0.2483	1.323	1.278
2.50	1082.6	0.2076	0.949	0.904
2.75	912.6	0.1636	0.643	0.598
3.00	785.8	0.1197	0.415	0.370
3.25	702.2		0.264	0.219
3.50	649.3		0.169	0.124

TABLE C 23

Run No. 23
 Air relative humidity 40 percent
 Air velocity 122 m/min
 Apple slice thickness 6.4 mm
 Type of tray plastic-coated, wire tray

TIME	WEIGHT	RATE	X_T	X
0.00	4873.9		7.271	7.174
0.10	4806.3	0.2675	7.156	7.059
0.15	4754.5	0.2727	7.068	6.971
0.20	4705.4	0.2779	6.985	6.888
0.25	4660.3	0.2794	6.908	6.811
0.30	4603.2	0.2801	6.811	6.714
0.35	4554.1	0.2823	6.728	6.631
0.40	4506.4	0.2750	6.647	6.550
0.45	4454.6	0.2763	6.559	6.462
0.50	4405.5	0.2778	6.476	6.379
0.60	4306.0	0.2745	6.307	6.210
0.65	4256.9	0.2680	6.224	6.126
0.70	4207.8	0.2602	6.140	6.043
0.75	4162.7	0.2602	6.064	5.967
0.80	4118.9	0.2609	5.989	5.892
0.85	4067.1	0.2654	5.902	5.804
0.90	4020.7	0.2676	5.823	5.726
0.95	3972.9	0.2588	5.742	5.645
1.00	3925.2	0.2557	5.661	5.564
1.10	3837.6	0.2507	5.512	5.415
1.25	3700.9	0.2505	5.280	5.183
1.50	3474.0	0.2472	4.895	4.798
1.75	3253.7	0.2373	4.521	4.424
2.00	3042.7	0.2254	4.163	4.066
2.67	2545.1	0.2059	3.319	3.222
3.00	2290.3	0.1953	2.887	2.789
3.50	1948.0	0.1808	2.306	2.708
4.00	1644.1	0.1578	1.790	1.693
4.50	1373.4	0.1348	1.331	1.233
5.00	1157.1	0.1074	0.964	0.866
5.50	978.0	0.0802	0.660	0.562
6.40	822.7		0.396	0.299
8.90	656.8		0.115	0.017

TABLE C 24

Run No. 24
Air relative humidity 10 percent
Air velocity 244 m/min
Apple slice thickness 6.4 mm
Type of tray plastic-coated, wire tray

TIME	WEIGHT	RATE	X_T	X
0.00	4619.9			
0.05	4444.4	1.2618	7.000	6.978
0.10	4216.4	1.2208	6.722	6.700
0.17	3929.8	1.1662	6.327	6.305
0.20	3801.2	1.1343	5.830	5.809
0.25	3590.6	1.0808	5.238	5.216
0.30	3400.6	1.02703	4.904	4.882
0.35	3231.0	0.9539	4.610	4.588
0.45	2903.5	0.8614	4.043	4.021
0.50	2748.5	0.8114	3.770	3.748
0.75	2114.0	0.6418	2.666	2.644
1.00	1602.3	0.5074	1.775	1.753
1.25	1207.6	0.3821	1.086	1.064
1.50	918.1	0.2609	0.580	0.558
1.75	735.8	0.1550	0.261	0.239
2.00	663.7		0.129	0.107
2.75	637.4		0.084	0.062

APPENDIX D

EXPLANATION OF THE COMPUTER PROGRAM USED TO SIMULATE THE DEHYDRATOR
DRYING PROCESS

The time allocated for each simulated tray was one tenth of the total drying time. Furthermore, this period was divided into 500 equal intervals and drying considered during these short time intervals. The program had the facility to compute the drying rate in each of any number of imaginary sections into which the tray was subdivided (the number of tray sections used, was set by program input specifications). Thus drying could be considered over a differential length of tray.

Since the drying tunnel being simulated is virtually adiabatic, the heat content of one gram of gas remains constant throughout the tunnel length:

$$T_1(0.24 + 0.46 Ha_1) + D Ha_1 = \text{constant} \quad (D.1)$$

Thus, by substituting the input conditions, to a section, of absolute humidity, Ha_1 , and temperature, T_1 , as well as the output humidity, Ha_2 , the value of the output temperature, T_2 , from that section, could be determined.

$$T_2(0.24 + 0.46 Ha_2) + D Ha_2 = T_1(0.24 + 0.46 Ha_1) + D Ha_1$$

or
$$T_2 = \frac{T_1(0.24 + 0.46 HA) - D(Ha_2 - Ha_1)}{(0.24 + 0.46 Ha_2)} \quad (D.2)$$

Before Eqn. (D.2) may be applied, the output absolute humidity has to be evaluated; it is done as follows:

$$Ha_2 = Ha_1 + (\text{accumulation due to drying}) \quad (D.3)$$

To determine the value of the accumulation term in Eqn. (D.3), the drying rate, $\frac{dw}{dt}$, had to be computed from an equation of the form:

$$\frac{dw}{dt} = A[0.01(Hr^* - Hr)ps]^B X_T^C \quad (9)$$

The values of the coefficients A, B and C are given in section 5.5, for different apple slice thicknesses.

The vapour pressure, ps (mm mercury), for any dry-bulb

temperature, T (degrees centigrade), was calculated from the following equation:

$$ps = \exp. \left[\frac{-5131.45}{T+293.15} + 20.3967 \right] \quad (D.4)$$

The value of the total moisture content of the apple rings, X_T , was known and Hr^* was calculated from:

$$Hr^* = \frac{356.06X_T^* + 5494.7X_T^{*2}}{1 + 6.123X_T^* + 54.437X_T^{*2}} \quad (13)$$

Since the air humidity was expressed as an absolute humidity, Ha [g water/g dry air], the percentage relative humidity, Hr , for Eqn. (9) was computed from the mole fraction of water in the air, y , the vapour pressure of water, ps , and the atmospheric pressure (taken as 760 mm mercury).

$$\therefore Hr = (y760/ps)100 \quad (D.5)$$

$$\text{but } y = 0.0555 Ha / (0.0555Ha + 0.0345) \quad (D.6)$$

substituting Eqn. (D.6) into (D.5) gives

$$Hr = 4218 Ha / [(0.0555Ha + 0.0345)ps] \quad (D.7)$$

Thus the values of X_T , Hr , Hr^* and ps may be substituted in Eqn. (9) to give the drying rate, $\frac{dw}{dt}$, of the tray section being considered. The accumulation term of Eqn. (D.3) is then given by:

$$\text{accumulation (of water) due to drying} = \frac{\left(\frac{dw}{dt}\right)(\text{tray section area})}{(\text{air mass flow rate})} \quad (D.8)$$

The moisture content of the apple rings after the drying interval is given by:

$$X_{T_{i+1}} = X_{T_i} - \left(\frac{dw}{dt}\right)(\text{time interval})/D \quad (D.9)$$

Note, D is [g bone-dry apple/m²].

Therefore the output absolute humidity, Ha_2 , and the air temperature, T_2 , may be computed by the above technique, as well as the total moisture content of the apple rings, after the drying interval.

In this manner, drying is considered 500 times for each tray section and for all of the 10 simulated tray positions.